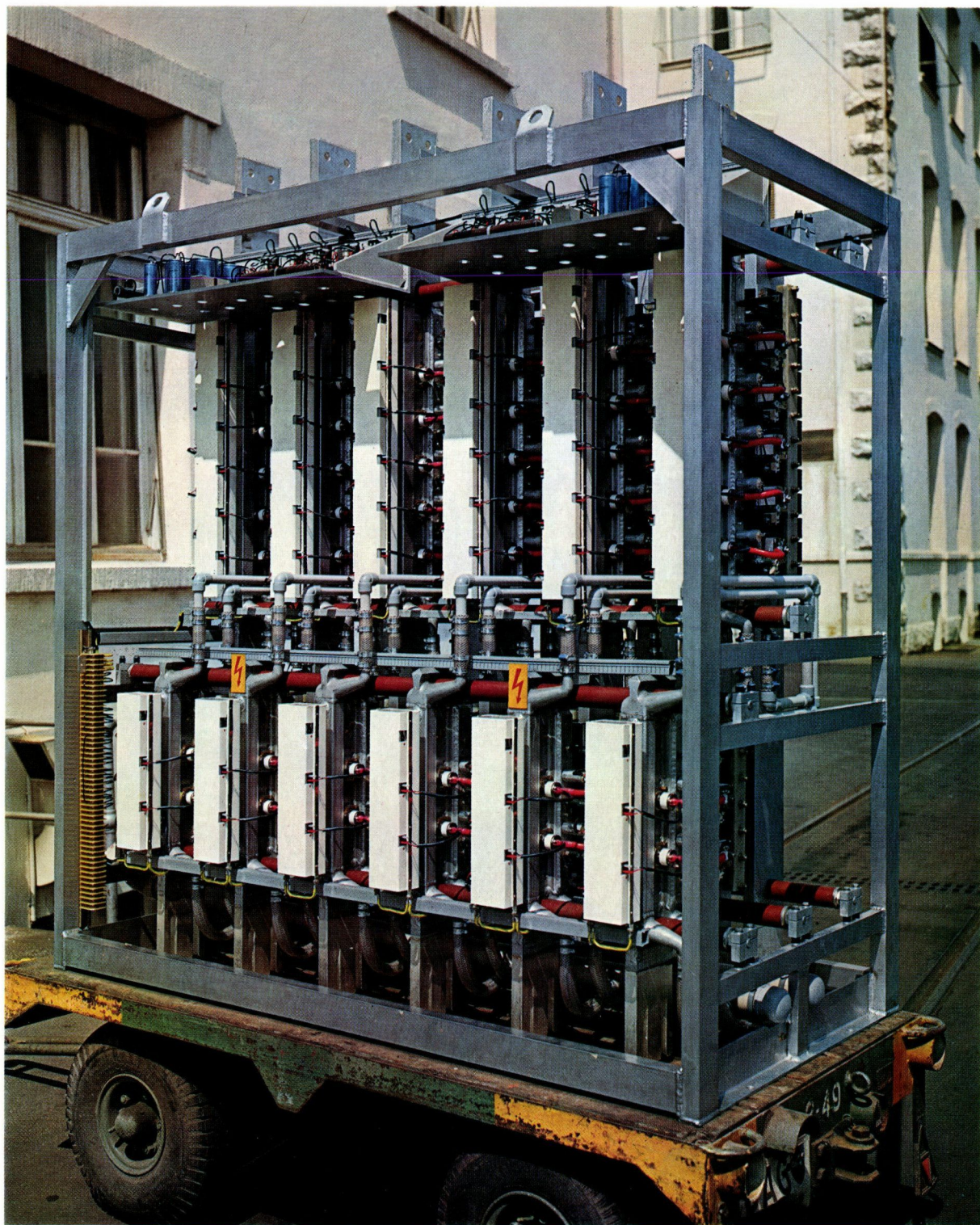


BROWN BOVERI REVIEW



BROWN BOVERI

143 471 - C

ISSUED BY BROWN, BOVERI & COMPANY, LIMITED, BADEN (SWITZERLAND)

No. 10

The Brown Boveri Review appears monthly — Reproduction of articles or illustrations is permitted subject to full acknowledgement

	Page		Page
M.Canay/L.Werren: Interrupting Sudden Asymmetric Short-Circuit Currents Without Zero Transition	484	M.Dick: High-Voltage Rectifiers for Large Transmitters	510
H.Ungrad/V.Narayan: Behaviour of Distance Relays Under Earth Fault Conditions on Double-Circuit Lines	494	P.Wolf: Digital Path Simulator for Conveyor Systems	520
E.Keller/M.Quisek: Thyribloc—A New Range of Liquid-Cooled Thyristor Converters . . .	502	B.Gänger/G.Maier: The Resistivity of Insulating Oil in a Direct-Voltage Field	525
		H.Strupp: The Accuracy of Calorimetry in Air Flow Measurement	534

Liquid-cooled thyristor converter of the Thyribloc range, d.c. rating 15 000 A

Interrupting Sudden Asymmetric Short-Circuit Currents Without Zero Transition

621.316.57.014.334.064.1

It is possible for the stator current of synchronous machines to be displaced completely to one side of the zero line for several cycles during sudden short circuits. In this article the time during which the curve does not pass through zero is calculated approximately with respect to the characteristics of the machine. The operating condition of the machine before the short circuit plays a considerable part and this is fully taken into account. A comparison of the various faults shows that the triple-pole terminal short circuit is the worst condition.

It is also shown that the interruption of a phase passing through zero effected by a breaker opening during a fault of this type results in a reduction of the d.c. in the residual circuit. Where the characteristics of the machine are normal and if the switching process is carried out at the correct time, this reduction is sufficient to cause the current in the residual circuit to immediately pass through zero and therefore the breaker can make a safe three-phase interruption.

It is known that sudden short-circuit currents in synchronous machines can be completely displaced to one side of the zero line, i.e. do not pass through zero, for several cycles. Certain standards [1] also acknowledge this phenomenon. It occurs far more readily and continues for much longer, the larger the d.c. component, and the greater the ratios of the time constants T_a/T_d'' and the reactances x_d'/x_d'' .

Also, a base load with a wide load angle or with underexcitation has a detrimental effect [2]. Amongst

other things Fig. 1a contains an oscillogram of a phase current I_U under a three-phase short circuit at a turbogenerator running under no load. The d.c. component has virtually the maximum possible value and as a result the curve does not reach the zero line until the 23rd cycle after the short circuit commenced. Fig. 1b shows the oscillogram of a test carried out on the same machine during which it was short circuited with no excitation and with a load angle of $\delta = 90^\circ$. The effect of the quadrature axis can be clearly seen.

The objects of this article are twofold:

- To derive quantitative information on the duration of these displaced currents in relation to the reactances and time constants of the machine and its operating condition before the short circuit. This enables us to determine whether the natural trend of machine characteristics towards higher outputs and greater utilization will lead to an increase in the duration of the displaced current.
- The phenomena occurring when the breaker trips and during the subsequent interruption of the current in one phase as it passes through zero are investigated. This will enable the true unsymmetry of the current for tripping the breaker to be evaluated.

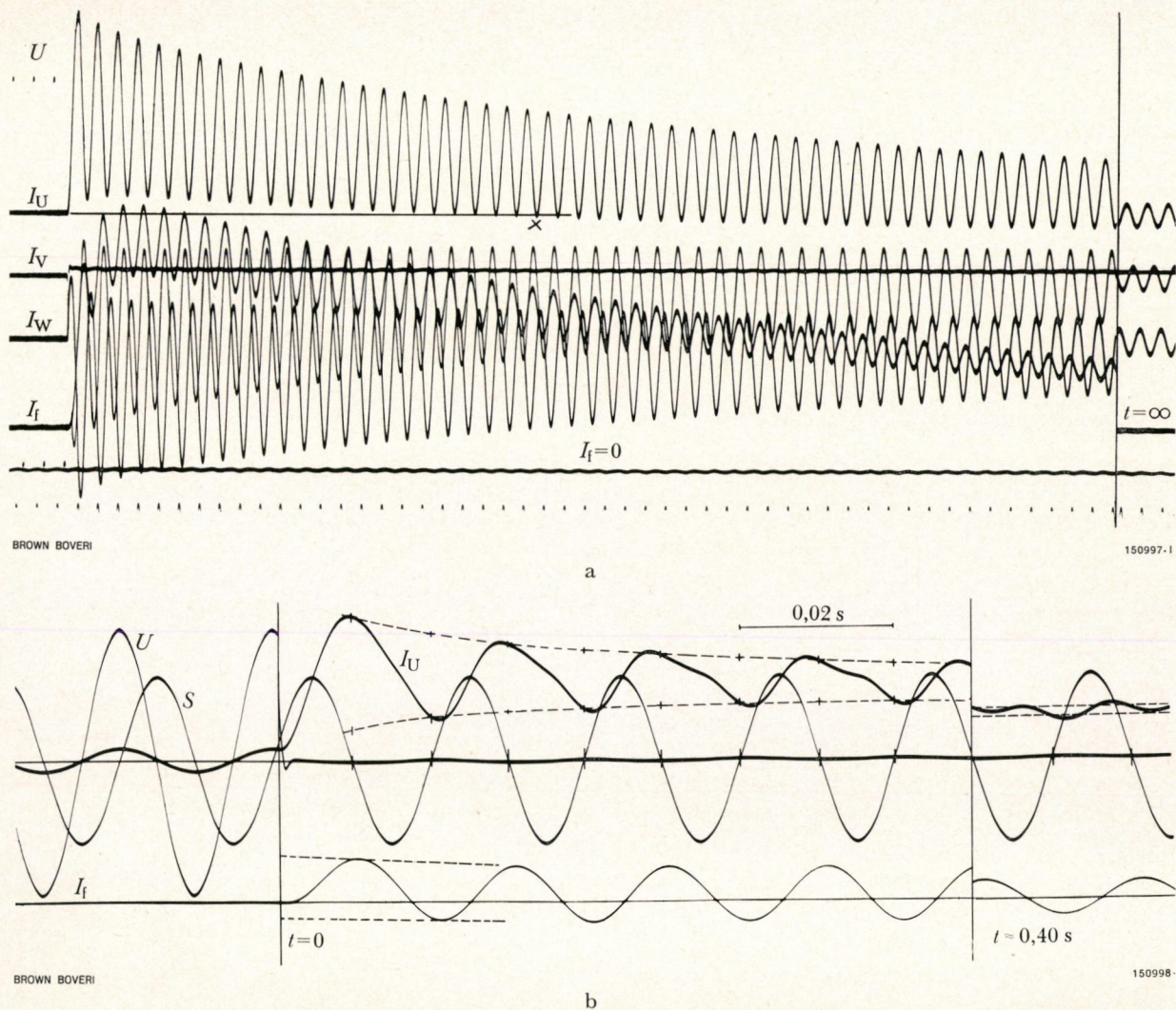


Fig. 1. - Oscillogram of a three-phase short circuit at a 230 MVA turbogenerator

a: Short circuit after no-load running

b: Short circuit with underexcitation and load angle $\delta = 90^\circ$

I_U, I_V, I_W = Stator currents

I_f = Rotor current

S = Signal voltage for determining rotor position

U = Stator voltage

x = First zero transition of current I_U

Causes of Sudden Displaced Short-Circuit Currents

The stator currents of synchronous machines under sudden short-circuit conditions are best illustrated by the locus diagram of the stator current phasor [3]. The instantaneous value of a phase current can be found by projecting the phasor i in the system of stator coordinates to the axes of the phases. The total stator current phasor comprises a rotating phasor,

i.e. the a.c. component i_{\sim} which decays with the a.c. time constants T'_d and T''_d and corresponds to the alternating currents in the phases, and a static d.c. component i_{-} which corresponds to the direct currents in the phases and which decays with the d.c. time constant T_a . For as long as the locus diagram of the stator current phasor is completely displaced to one side of a straight line perpendicular to any one of the phase axes, the current in this phase does not pass through zero. The locus diagram of a

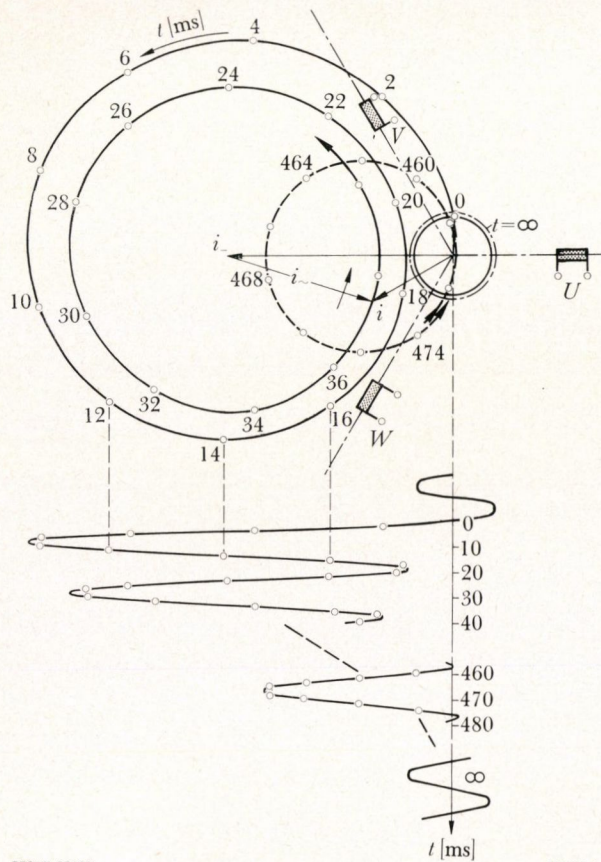


Fig. 2. - Locus diagram of stator current phasor for a 400 MVA turbogenerator

$T_a = 0.53 \text{ s}$	$x_d = 2.56$
$T'_d = 1.30 \text{ s}$	$x'_d = 0.03$
$T''_d = 0.03 \text{ s}$	$x''_d = 0.22$
$T'_q = T''_d$	$x_q = 2.43$
	$x''_q = x''_d$

U, V, W = Axes of stator windings

i_- = D.C. component of stator current phasor

i_{\sim} = A.C. component of stator current phasor

i = Total stator current phasor

400 MVA machine under short circuit after operating at rated active load and a power factor of 1 is shown in Fig. 2. The short circuit was timed to coincide with maximum possible d.c., that is exactly i_- , in phase U . This particular case is the example used throughout the following. A current does not pass through zero for as long as its d.c. component is larger than the amplitude of the a.c. component i_{\sim} . As the axis of the d.c. phasor cannot be more than 30° from that of one of the three phases, at whatever phase position the d.c. component is in, i.e. at whatever point in time, the short circuit is instigated, one of the three phases is carrying a direct current of at least 86.6% of the d.c. component i_- .

With a three-phase short-circuit at a machine running under no load, i_- and i_{\sim} are equal at $t = 0$ (Fig. 3a). Alternating current i_{\sim} decays initially with the time constant T''_d and because $T''_d < T_a$ the value of i_{\sim} is at first smaller than i_- which

decays with T_a . It is not until after a certain time T has elapsed that the first passage through zero occurs, because now i_{\sim} decays with time constant T'_d ($T'_d > T_a$) and becomes greater than i_- .

In order to illustrate the effect of a steady-state load before the short circuit, the current curves for three typical operating conditions (Fig. 3b, 3c and 3d) were calculated for the 400 MVA machine mentioned above. It can be clearly seen from the illustrations that operating with a wide load angle (Fig. 3c) or underexcitation (Fig. 3d) causes the first zero transition to be much later than is the case with a machine running under no load. In the first case the increase in time where no zero transitions occur is a result of the large quadrature axis component with subtransient decay and in the second case it is because of the diminished initial value of the alternating current. Because of the higher initial a.c., a short circuit under rated service

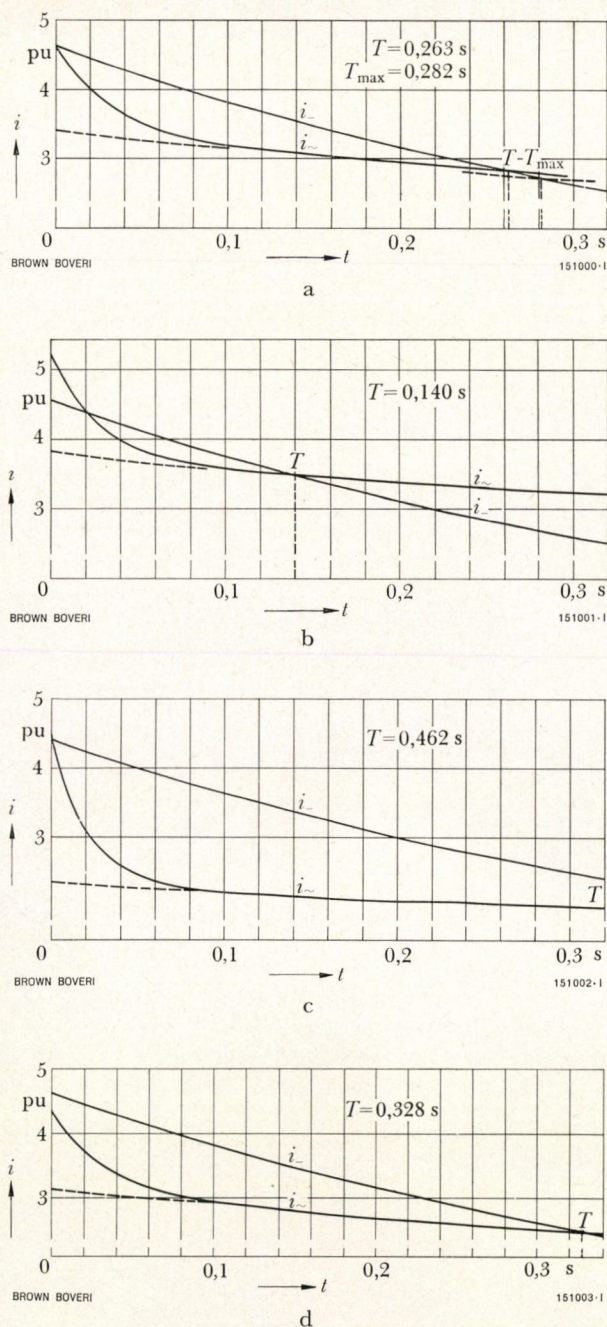


Fig. 3. — Curves of d.c. and a.c. for short circuit after various steady-state operating conditions of a 400 MVA turbogenerator

- a: No load
 b: Rated load, $I = 1.0$ p.u., p.f. = 0.75
 c: Rated active load, $I = 0.745$ p.u., p.f. = 1.0
 d: Capacitive load, $I = 0.25$ p.u., p.f. = 0

i_{\sim} = A.C. component (amplitude)

i_{-} = D.C. component

T = Time of first zero transition

T_{\max} , see Eq. (1)

All other data as Fig. 2.

conditions (Fig. 3b) is more favourable with regard to the current passing through zero. In this case the curve passes through zero immediately after the short circuit commences but the rapid decay of the subtransient component means that after the first cycle the short-circuit current no longer reaches the zero line.

Duration of Displaced Short-Circuit Currents with Three-Phase Short Circuits

If we limit the calculation to times $t \geq T_d''$ and T_q'' (practical limit about $t \geq 3 T_d''$) all subtransient currents can be disregarded. The alternating current is shown in Fig. 3a, 3b, 3c and 3d and where this subtransient component is disregarded the a.c. is shown dotted. This reduction is justifiable because the cases we are concerned with are those where the current does not pass through zero for a considerable time ($t > 0.1$ s). We can therefore assume

$$T_d'' = T_q'' = 0$$

and also that

$$x_d'' = x_q''$$

i.e. that the machine is symmetrical in the subtransient range.

With an asymmetrical machine ($x_q'' \neq x_d''$) and an asymmetrical short-circuit current, an a.c. component with double the basic frequency occurs and this also decays with the time constant T_a of the d.c. component. We can therefore regard this a.c. together with the d.c. component as a pulsating d.c. With a short circuit after no-load running and in the case of $x_q'' > x_d''$, the short-circuit current peaks near the zero line are flattened by the second harmonic and the peaks on the other side are raised. This appears to encourage the lack of zero transitions. It should be noted however, that the maximum values of the pulsating d.c. are exactly the same as those of the non-pulsating d.c. which is derived from our assumption that $x_q'' = x_d''$ (Fig. 4). The a.c. reaches its peak value at exactly the same time as the pulsating d.c. reaches its maximum value ($t = 1, 2, 3 \cdot \pi$ rad) and therefore the peaks of the actual current with the second harmonic and the peaks of the current calculated under the assumption that $x_q'' = x_d''$ are exactly the same distance from the zero

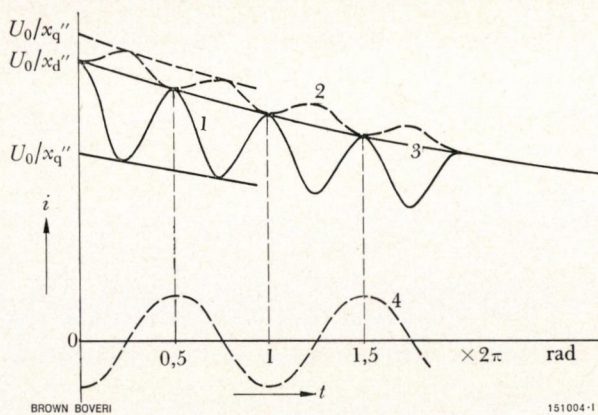


Fig. 4. – Second harmonic of short-circuit current after no-load running

- 1 = Pulsating d.c. at $x_q'' > x_d''$
- 2 = Pulsating d.c. at $x_q'' < x_d''$
- 3 = Pure d.c. at $x_q'' = x_d''$
- 4 = A.C. (schematic to illustrate phase positions)

line. A short circuit on a machine which is preloaded does not change the amplitude of the purely d.c. component or the second harmonic, but the preload does affect the phase displacement of the latter [4]. If we use $x_q'' = x_d''$ for calculating approximately the time T to the first pass through zero, we obtain an upper limit value because instead of using the true pulsating d.c. (curve 2, Fig. 4) we are using its upper envelope (curve 3) which is a higher value.

In a few rare cases x_q'' can be less than x_d'' in the range where x_q''/x_d'' is between 0.9 and 1.0. In this case the peaks near the zero line become more prominent and the opposite ones flattened during a short

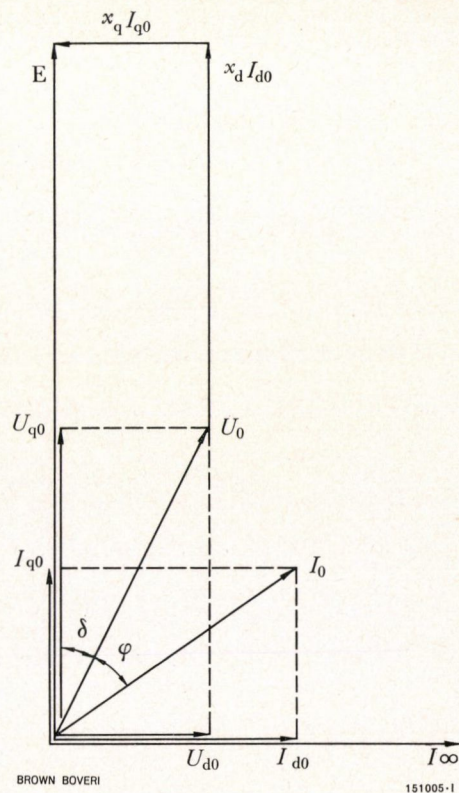


Fig. 5. – Vector diagram of a synchronous machine in steady-state operation

- E = Synchronous internal voltage
- I_0 = Armature current before short circuit
- I_{d0} = Direct-axis component of I_0
- I_{q0} = Quadrature-axis component of I_0
- I_∞ = Armature current under sustained short circuit
- U_0 = Terminal voltage before short circuit
- U_{d0} = Direct-axis component of U_0
- U_{q0} = Quadrature-axis component of U_0
- δ = Load angle
- φ = Phase angle

Duration of displaced short-circuit current under various operating conditions

Preload	No load $I = 0$	Rated load $I = 1$ [p.u.] p.f. = 0.75	Rated active load $I = 0.745$ [p.u.] p.f. = 1.0	Capacitive load $I = 0.25$ [p.u.] p.f. = 0
Figures	3a	3b	3c	3d
T (read from illustrations) [s]	0.263	0.140	0.462	0.328
T_{\max} (from Eq. (1)) [s]	0.282	0.187	0.684	0.345

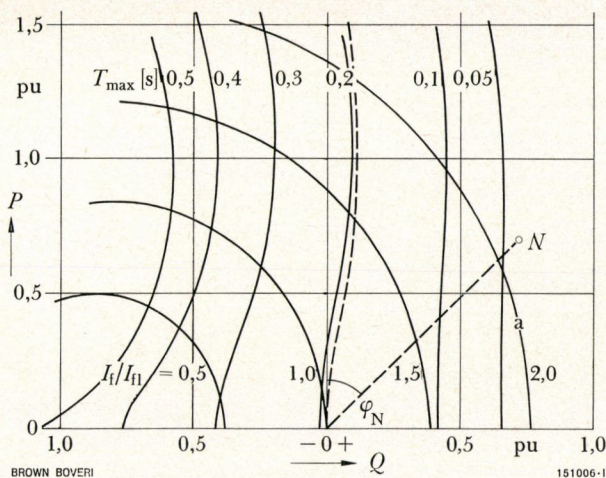


Fig. 6. - T_{\max} in relation to preload for a 60 MVA, 375 rev/min salient pole generator

a = Curves of constant excitation	$T_a = 0.50$ s
I_{f1} = Excitation current at no load	$T'_d = 1.40$ s
I_f = Excitation current under load	$T''_d = 0.032$ s
N = Point of rated operation	$x_d = 1.31$
P = Active load	$x'_d = 0.31$
Q = Reactive load	$x''_d = 0.24$
	$x_q = 0.87$

circuit after no load running. The distances from these peaks to the zero line are also identical to those of the peaks of the short-circuit currents calculated according to $x''_q = x''_d$. Assuming $x''_q = x''_d$ for a short circuit at a loaded machine, this gives us a value for T which is somewhat too small because the d.c. used in the calculation is smaller than the actual pulsating current. The error is acceptable, however, because x''_q is never appreciably smaller than x''_d .

Under the above assumptions the stator current comprises the following two components (cf. Fig. 5)

$$i_{\sim} = I_{d0} + U_{q0} \left[\left(\frac{1}{x'_d} - \frac{1}{x_d} \right) e^{-t/T'_d} + \frac{1}{x_d} \right]$$

with
$$I_{d0} = \frac{E - U_{q0}}{x_d}$$

and
$$i_{-} = \frac{U_0}{x'_d} e^{-t/T_a},$$

where from $t > 0$ upwards $i_{\sim} > i_{-}$ because the subtransient a.c. component has already been neglected. At time $t = T$ at the first zero transition these components are equal in magnitude

$$\frac{E}{x_d} + U_{q0} \left(\frac{1}{x'_d} - \frac{1}{x_d} \right) e^{-t/T'_d} = \frac{U_0}{x'_d} e^{-t/T_a}$$

In order to derive a finite solution we can substitute the smaller value $E/x_d e^{-t/T'_d}$ for $E/x_d = I_{\infty}$, i.e. one imagines that the sustained short-circuit current I_{∞} which is relatively small in the time range with which we are concerned here also decays with T'_d . From this we can obtain an upper limit for T (Fig. 3a)

$$T_{\max} = \frac{T'_d T_a}{T'_d - T_a} \ln \left[\frac{x'_d}{x''_d} \frac{U_0}{U_{q0} + I_{d0} x'_d} \right] \quad (T_{\max} \gg T'_d, T''_d) \quad (1)$$

Values U_{q0} and I_{d0} have to be taken from the phasor diagram for steady-state operation (Fig. 5) or calculated.

The Table on p. 488 gives values for the duration of a displaced short-circuit current. These were obtained with the 400 MVA machine in the four operating conditions of Fig. 3a to 3d.

The direct influence of ratio x'_d/x''_d and time constants T_a and T'_d is illustrated by Eq. (1). The effect of the preload is given by the factor $U_0/(U_{q0} + I_{d0} x'_d)$. Operation with a large load angle or capacitive reactive load leads to an additional increase in the duration of a displaced short-circuit current.

Each pair of values of U_{q0} and I_{d0} corresponds unequivocally to an operating point in the power diagram. This interrelationship permits the curves $T_{\max} = \text{constant}$ to be drawn in the current or power diagram. The effect of the preload is easy to see from the graphs.

The family of curves $T_{\max} = \text{constant}$ has the characteristic that two curves $T_{\max 1}$ and $T_{\max 2}$ intersect the same line segment of each straight line for $\delta = \text{constant}$ where $\delta = \text{load angle}$. It is a simple matter to derive the segments on the straight line curve $\delta = 0$. The complete diagram can then be drawn using these and a single, complete curve for T_{\max} .

The loci of $T_{\max} = \text{constant}$ for a medium sized salient pole machine (60 MVA) are shown in Fig. 6. When operating at rated power T_{\max} is much smaller than the already low value of 0.19 s for no-load operation. The value of T_{\max} for a short circuit after no-load running is therefore not representative. The increase in T_{\max} with underexcitation is obvious but in this particular example the effect of the active power is very small because of the low value of x_d .

The conditions for a 750 MVA turbogenerator are shown in Fig. 7a. Because of the small difference

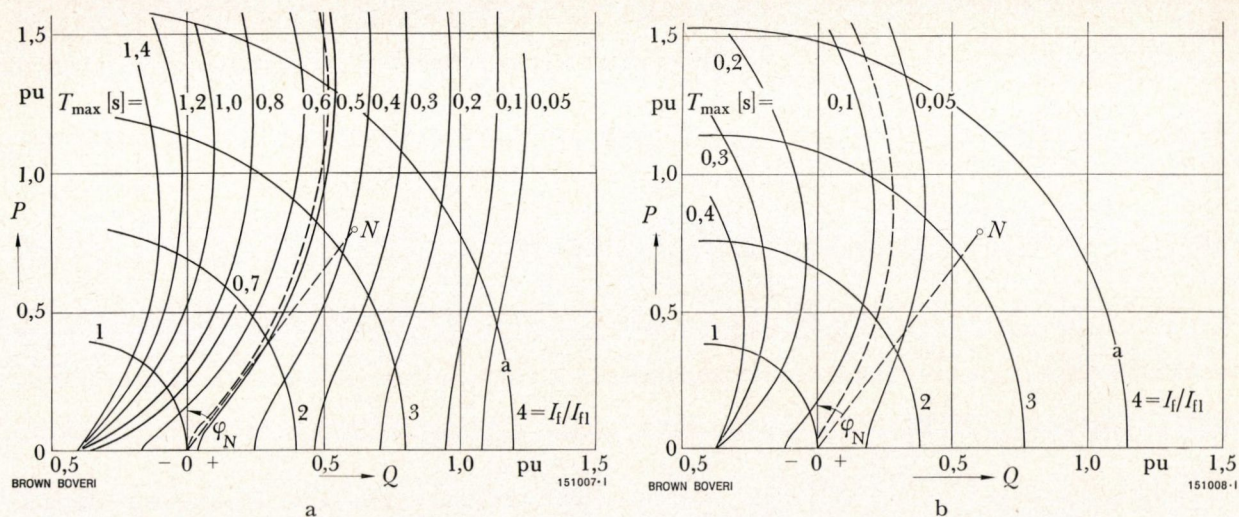


Fig. 7.— T_{\max} in relation to preload for a 750 MVA, 3000 rev/min turbogenerator

a: Short circuit at terminals

b: Short circuit after a transformer in unit connection

Generator data: $T_a = 0.63$ s $x_d = 2.50$
 $T'_d = 1.05$ s $x'_d = 0.32$
 $T''_d = 0.026$ s $x''_d = 0.23$

Transformer data: $r_k = 0.003$ $x_k = 0.145$

a = Curves of constant excitation
 I_{f1} = Excitation current at no load
 I_f = Excitation current under load
 N = Point of rated operation
 P = Active load
 Q = Reactive load

between T'_d and T_a the value T_{\max} is generally high and the load angle and underexcitation have very pronounced effects.

Values of the Characteristic Quantities of Synchronous Machines

The normal ranges of values of the characteristic quantities of synchronous machines are compiled in the following Table for reference.

Quantity	Turbo-generators	Salient pole generators
x_d [p.u.]	1.0 – 2.7	0.6 – 1.6
x'_d [p.u.]	0.12 – 0.45	0.18 – 0.5
x''_d [p.u.]	0.08 – 0.30	0.11 – 0.35
T_d [s]	0.6 – 1.5	0.5 – 3.0
T'_d [s]	0.01 – 0.06	0.01 – 0.10
T_a [s]	0.06 – 0.80	0.05 – 0.6

The following can be said of the trend of the characteristic quantities as unit outputs continue to increase:

- Higher electrical utilization leads to increased reactances.
- Increasing machine output naturally results in an increase in T_a to about 0.8 s at outputs of 800 MVA and about 0.4 s for short circuits on the high voltage side of the generator transformer [1].
- When the excitation windings have direct liquid cooling T'_d will become smaller.

The last two considerations will both lead to an increase in the duration of a displaced short-circuit current.

Short Circuit after the Generator Transformer

If there is an additional impedance x_e , such as a generator transformer, between the location of the short circuit and the machine, the values

$$x_{d\text{tot}} = x_d + x_e, \quad x'_{d\text{tot}} = x'_d + x_e, \quad x''_{d\text{tot}} = x''_d + x_e$$

which are increased by the external reactance x_e must be substituted for the reactances in Eq. (1). The transient short-circuit time constant is also affected as follows

$$T'_{d\text{tot}} = T'_{d0} \frac{x'_{d\text{tot}}}{x_{d\text{tot}}} = T'_d \frac{x_d}{x'_d} \frac{x'_{d\text{tot}}}{x_{d\text{tot}}} \quad (2)$$

With a short circuit after the generator transformer, its short-circuit reactance x_k (where $x_e = x_k$) reduces the ratio x'_d/x_d and increases time constant T'_d . On the other hand the time constant $T_{a\text{tot}}$ is smaller than T_a because the resistance of the transformer is relatively greater than that of the machine ($r_k/x_k > r_a/x_2$). The governing expression $T_a T'_d / (T'_d - T_a)$ becomes smaller and the time T_{max} noticeably shorter. In other words the asymmetry decays more quickly and the d.c. more slowly; the subtransient component of the a.c. has become relatively smaller. All these changes have the overall effect that the current passes through zero much sooner. The loci of T_{max} for the same machine with a short circuit after the generator transformer are shown in Fig. 7b for comparison with Fig. 7a. It can be seen that the values of T_{max} are reduced to about one sixth.

Line-to-Line and Line-to-Earth Faults

These conditions can be related to the three-phase fault by the method of symmetrical components. The total reactance of the positive sequence system for a line-to-line fault is series connection of the positive sequence and negative sequence reactance but in the case of a line-to-earth fault zero sequence reactance must be included. In the same manner as with a fault, after a generator transformer, equal reactances are added to the machine reactances x'_d and x''_d . The d.c. time constant can also be determined approximately from the total subtransient positive sequence reactance [5, 6]. The effects on T_{max} are the same as with a short circuit after the generator transformer. A line-to-line or line-to-earth fault does not affect T_{max} as much as a three-phase one. For example the following T_{max} values apply for a 750 MVA machine at various fault conditions after no-load running using the approximate values $x_2 \approx x'_d$ and $x_0 \approx x''_d/2$:

Type of fault	Three-phase	Three-phase	Line-to-line	Line-to-earth
Location	Terminals	After transformer	Terminals	Terminals
T_{max} [s]	0.52	0.08	0.19	0.11

Current Characteristics when the Breaker Opens

Previous considerations were based on a current characteristic for an uninterrupted short circuit, as is well known from oscillograms of short-circuit testing. In practice the breaker will open after a certain time. The behaviour of the machine during this switching sequence is therefore important for the interruption to succeed.

Three-Phase Fault

The most unfavourable current characteristic with maximum possible d.c. which has always been considered up till now, can occur in only one phase. The other two phases carry half the d.c. each so that in practical cases these phase currents pass through zero from the beginning. In the other limiting case 86.6% of the maximum d.c. flows in two phases and the current in the third is then fully symmetrical.

One phase is interrupted by the breaker as the current passes through zero. The question is: how much of asymmetry remains in the circuit immediately after the interruption? It is assumed that the a.c. component in one phase remains very nearly unchanged after interruption. As, at the time in question, $t > 0.1$ s this current is already lower than the a.c. of a fault which from the outset is only line-to-line, and, as time increases, will attain the same value, this assumption is on the safe side.

After the interruption only the $i_{-(UW)}$ component of the stator d.c. i_- , can be maintained. This component lies in the direction of the new combined phase (UW) in Fig. 8. In accordance with the assumptions the current vector i_- lies in the direction of U . The component in the direction of (UW) is $i_- \cos 30^\circ$. The residual d.c. in phases U and W are therefore $\pm i_- \cos^2 30^\circ = \pm 3/4 \cdot i_-$, i.e. 25% lower.

If, therefore, the residual current in the two-phase short-circuit loop must immediately pass through zero, the following condition must apply

$$\frac{3}{4} i_- < i_{\sim}$$

If once again we substitute $\frac{U_0}{x_d} e^{-t/T_d'}$ for $\frac{U_0}{x_d}$, for short circuit after no load we have

$$\frac{3}{4} \frac{U_0}{x_d'} e^{-t/T_a} < \frac{U_0}{x_d'} e^{-t/T_d'} \quad (3)$$

$$\frac{x_d'}{x_d''} < \frac{4}{3} e^{\left(\frac{1}{T_a} - \frac{1}{T_d'}\right)t}$$

The ratio x_d'/x_d'' is between 1.3 and 1.5 (and in certain cases higher) and is reduced if transformer reactances are taken into account.

Where $x_d'/x_d'' < 4/3$ the above condition is fulfilled as from $t = 0$ because under normal circumstances $T_a < T_d'$. Where $x_d'/x_d'' > 4/3$, condition (3) is fulfilled only as from the critical time $t = T_K$

$$T_K = \frac{T_d' T_a}{T_d' - T_a} \ln \left(\frac{3}{4} \frac{x_d'}{x_d''} \right) \quad (4)$$

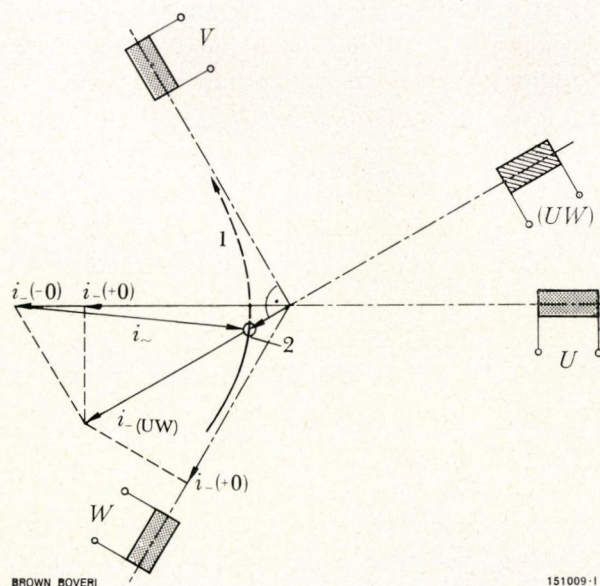


Fig. 8. — Stator current phasor when interrupting a phase current (derived from Fig. 2)

- 1 = Locus of stator current vector
- 2 = Time when current in phase V is interrupted
- i_- = D.C. component before interruption
- $i_-(UW)$ = D.C. component after interruption
- i_{\sim} = A.C. component (remains unchanged)

In all practical cases T_K is less than the switching delay and therefore the breaker has also to interrupt currents which pass through zero in the remaining phases. For the 750 MVA machine (Fig. 7a and 7b) the critical time $T_K = 0.068$ s, which is considerably less than the minimum switching delay which is about 0.1 s.

With a short circuit in steady-state operation the factor $U_0 / (U_{q0} + I_{d0} x_d')$ must be incorporated in the logarithmic argument of Eq. (4) so that similar loci are derived for $T_K = \text{constant}$ to those for $T_{\max} = \text{constant}$.

Line-to-Line and Line-to-Earth Faults

With these faults there is no longer any favourable phase current which passes through zero and whose interruption also instigates interruption of the other phase currents. Also it is necessary to wait for the first actual zero transition to ensure safe interruption. Although this time is much shorter for a line-to-line fault than in the case of a three-phase one, if conditions are unfavourable and the fault is at the terminals it can be long enough to exceed the minimum response and could conceivably necessitate a delay of the switching operation. With a line-to-earth fault the first zero transition is much sooner than with a line-to-earth one and need therefore no longer be considered. The probability of a large asymmetry occurring is much slimmer with a line-to-line or line-to-earth fault than with a three-phase fault.

Conclusions

The above method for calculating approximately the maximum time T_{\max} taken for a sudden short-circuit current to pass through zero confirms numerically the well known observation that a short circuit after operation at rated output is less dangerous than after no-load running, but that previous operation with a large load angle or underexcitation leads to a considerable increase in T_{\max} . The natural trend towards increasing the armature time constant T_a with rising unit output, and reduction of the transient time constant T_d' with direct liquid cooling

in the rotor, results in an increase in T_{\max} . The worst fault condition is a three-phase short circuit at the terminals. With a line-to-line or line-to-earth fault or short circuits with additional reactances in the short-circuit loop, such as a transformer, T_{\max} becomes shorter. For example, in a large machine with a short circuit after no-load running T_{\max} is thus reduced from 0.52 to 0.08 s.

When the breaker opens following a three-phase short circuit and interrupts the phase current which passes through zero and is always present, the result is a reduction in the d.c. of the residual circuit, i.e. in the two adjacent phases. With normal values for the characteristic quantities of the machine and the time when switching takes place, this reduction is usually sufficient to cause the current in the residual circuit to pass through zero. This could be the reason why although short-circuit currents which do not pass through zero can easily occur in medium sized machines, this condition has not, as yet, presented any difficulties in interrupting it. In unfavourable

conditions, however, the line-to-line fault can demand a delay in the switching time.

(AH)

M. CANAY
L. WERREN

Bibliography

- [1] VDE 0102 Part 1/9.62. Leitsätze für die Berechnung der Kurzschlussströme, part 1, Drehstromanlagen mit Nennspannungen von 1 kV und darüber. VDE-Verlag, Berlin.
- [2] A. WEBS: Sonderprobleme bei Kurzschlüssen in Drehstromnetzen. VDE proceedings, Bremen 1966.
M. CANAY: Discussion.
- [3] M. CANAY: Ein neues Verfahren zur Bestimmung der Querachsengrößen von Synchronmaschinen. Elektrotech.Z. Series A, 1965, Vol. 86, No. 17, p. 561-8.
- [4] T. LAIBLE: Die Theorie der Synchronmaschine im nichtstationären Betrieb. Springer, Berlin/Göttingen/Heidelberg 1952.
- [5] C. CONCORDIA: Synchronous Machines. John Wiley & Sons, New York 1951.
- [6] K. BONFERT: Das Betriebsverhalten der Synchronmaschine. Springer, Berlin/Göttingen/Heidelberg 1962.

Behaviour of Distance Relays Under Earth Fault Conditions on Double-Circuit Lines

621.316.925.45

Mutual impedance in the zero sequence system prevents accurate measurement by distance relays during earth faults in double-circuit lines. Although it is relatively small, under certain circumstances this error can slightly delay the interruption of the faulty line. There are certain methods of compensation which ensure rapid interruption in the correct sequence. Under certain conditions, however, all these methods can lead to non-selective interruption of the sound line and for this reason it is not always desirable to provide such compensation. On the whole, compensation has more drawbacks than advantages and is in general not applied by us. Suitable coupling between the relays at both ends of the protected line permits immediate selective interruption of earth faults on the double-circuit line.

Measurement by distance relays in double-circuit lines of solidly earthed systems is affected by the mutual zero sequence impedance between the two lines. On the other hand the mutual positive and negative sequence impedances normally remain small. Since, transposing the conductors makes them very close to zero, they are negligible for practical purposes. Similar considerations apply for double earth faults in impedance-earthed systems.

Key to Symbols

A, B, C, D	Busbars
F	Location of single-phase earth fault
I_1, I_2, I_3	Current measured by relays 1, 2 and 3
I_1^R, I_2^R	Current in the faulted phase (relay 1 or 2)

$3 I_1^0, 3 I_2^0$	Summation current in the faulted line (relay 1 or 2)
$3 I_3^0, 3 I_4^0$	Summation current in the sound line (relay 3 or 4)
$k_0 = \frac{1}{3} \left(\frac{z^0}{z'} - 1 \right)$	Correction factor for summation current
l	Length of line
U_A^R, U_B^R, U_C^R	Phase voltage to earth at busbar A, B or C of the faulted phase
x	Distance between fault and busbar A
z^0	Zero sequence impedance of protected line [$\Omega/\text{ph km}$]
Z_C^0, Z_D^0	Zero sequence source impedances on busbars C or D
z'	Positive or negative sequence impedances of protected line [$\Omega/\text{ph km}$]
z^m	Mutual zero sequence impedance of the parallel lines [$\Omega/\text{ph km}$]
Z_1, Z_2, Z_3	Impedance measured by relays 1, 2 or 3
1, 2, 3, 4	Relays and associated circuit-breakers

Error in Measurement During Single-Phase Earth Faults

The effect of mutual zero impedance depends on its magnitude, the source impedances and the distribution of the earthing points. Two conditions are considered; supply at one end and at both ends of the line.

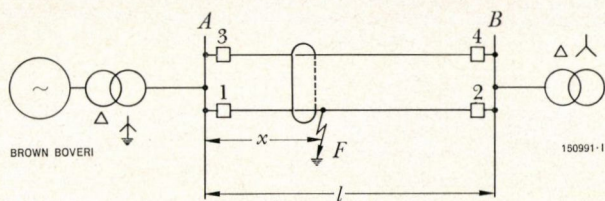


Fig. 1. - Double-circuit line with supply at one end only

A, B = Busbars

F = Location of single-phase earth fault

l = Length of line

x = Distance of fault from A

1, 2, 3, 4 = Relays

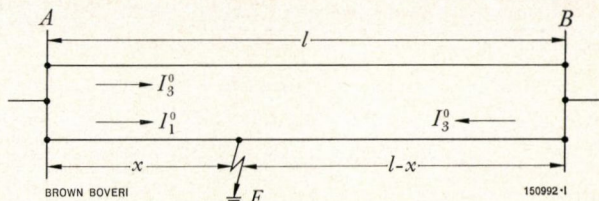


Fig. 2. - Currents in the faulted system (Fig. 1)

A, B = Busbars

F = Location of single-phase earth fault

I_1^0 = Current in faulted line

I_3^0 = Current in sound line

l = Length of line

x = Distance of fault from A

Supply at One End

This is illustrated by Fig. 1. The measured impedance of the usual type of distance relay is formed by the quotient

$$Z = \frac{U^R}{I_1^R + 3I_1^0 \cdot k_0}$$

The measuring voltage of the faulted phase at busbar A is

$$U_A^R = z' \cdot x \cdot (I_1^R + 3I_1^0 k_0) + I_3^0 \cdot z^m \cdot x$$

and the current in relay 1

$$I_1 = I_1^R + 3I_1^0 \cdot k_0$$

The impedance measured by relay 1 is

$$Z_1 = \frac{U_A^R}{I_1} = z' \cdot x + \frac{I_3^0 \cdot z^m \cdot x}{I_1^R + 3I_1^0 \cdot k_0}$$

and as $I_3^0 (2l - x) = I_1^0 \cdot x$ (see Fig. 2)

and $I_1^R = 3I_1^0$

becomes

$$Z_1 = z' \cdot x + \frac{z^m \cdot x \cdot z' \cdot [x/(2l - x)]}{2z' + z^0}$$

$$Z_1 = z' \cdot x \left[1 + \frac{z^m}{2z' + z^0} \cdot \frac{x}{2l - x} \right] \quad (1)$$

The impedance measured by relay 3 is

$$Z_3 = \frac{U_A^R}{I_3} = z' (2l - x) \left[1 + \frac{z^m}{2z' + z^0} \cdot \frac{x}{2l - x} \right] \quad (2)$$

Similarly the impedance measured by relay 2 is

$$Z_2 = \frac{U_B^R}{I_2} = z' (l - x) \left[1 - \frac{z^m}{2z' + z^0} \right] \quad (3)$$

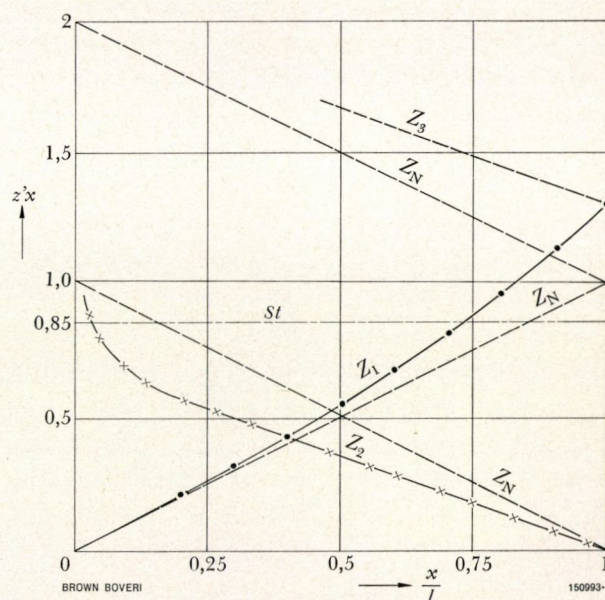


Fig. 3. - Impedances measured by the distance relays under earth fault on double-circuit line with supply at one end (Fig. 1)

l = Length of line

St = Step limit

x = Distance of fault from A

z' = Direct or indirect impedance in the protected line

Z_1 = Impedance measured by relay 1

Z_2 = Impedance measured by relay 2

Z_3 = Impedance measured by relay 3

Z_N = Line impedance ($z^m = 0.5 z^0$)

The second term of the expression in brackets in Eq. (1), (2) and (3) represents the error in measurement due to mutual zero impedance of the parallel lines.

The impedance measured by relays 1, 2 and 3 are shown in Fig. 3. These figures were derived for a system having values of $z^0 = 3 z'$ and $z^m = 0.5 z^0$ which are average in practice.

The error in measurement at relay 1 increases from 0 at $x = 0$ to about 30% at $x = l$ (fault at end of line). If the first step is set to 85% of the total length of line, the actual length of line covered is about 72%. On the other hand relay 2 responds in the first step for all single-phase faults on the protected line. Assuming that response sensitivity is infinite, the percentage error in measurement by relay 2 remains constant. It should be noted however, that the current flowing through relay 2 becomes smaller and smaller as x decreases. This means that there is a limit below which relay 2 will no longer respond with supply at one end only. Rapid tripping by relay 2 for single-phase faults along the whole length of the line does not indicate non-selectivity. As relay 3 always measures a larger impedance than that to the fault (measured from the relay), this again does not lead to non-selective interruption. A fault in the vicinity of relay 2 will be cleared by relay 3 in its second step.

Supply at Both Ends

In most cases double-circuit lines are fed at both ends. Even with supply at one end only it often happens that the transformer neutral points at both ends of the double-circuit lines are earthed. This means that the neutral current is supplied from both ends.

A common type of double-circuit line with supply from both ends and earthed neutral points is illustrated by Fig. 4.

The voltage to earth in the faulty phase at busbar C is

$$U_C^R = z' \cdot x [I_1^R + 3 I_1^0 \cdot k_0] + I_3^0 \cdot z^m \cdot x$$

and the impedance measured by relay 1

$$Z_1 = z' \cdot x \cdot \left[1 + \frac{I_3^0 \cdot z^m}{I_1^R z' + I_1^0 (z^0 - z')} \right] \quad (4)$$

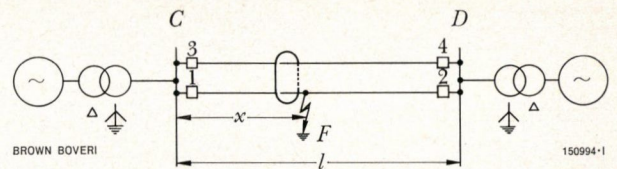


Fig. 4. - Double-circuit line with supply at both ends

C, D = Busbars

F = Location of fault

l = Length of line

x = Distance of fault from C

1, 2, 3, 4 = Relays and their breakers

Similarly the impedance measured by relay 2

$$Z_2 = z' \cdot x \cdot \left[1 + \frac{I_4^0 \cdot z^m}{I_2^R \cdot z' + I_2^0 (z^0 - z')} \right] \quad (5)$$

where

$$I_4^0 = - I_3^0$$

If the fault is near busbar C the zero sequence currents in relays 1 and 3 are opposed, whereas they have the same direction if the fault is near busbar D. Depending on the magnitude of the zero sequence source impedances and the mutual zero sequence impedance of the parallel lines the zero sequence current I_3^0 in the parallel healthy line will disappear for a particular value of x .

The measurement of a single-phase earth fault at this point will be exact and this fault location is given by

$$\frac{x}{l-x} = \frac{z^m \cdot x + Z_C^0}{z^m (l-x) + Z_D^0}$$

Depending on the fault location the value of I_3^0/I_1^0 will be between -1 and +1. For all faults to the left of the point where $I_3^0/I_1^0 = 0$, relay 1 will measure a smaller impedance, and for all faults to the right the impedance measured will be greater than the real value.

As illustrated by Eq. (4) and (5) the error increases with z^m . The main factors which determine the mutual zero sequence impedance of the parallel lines are the geometric arrangement, specific earth resistance, height of the lines above ground, number of earthing lines, frequency and so on.

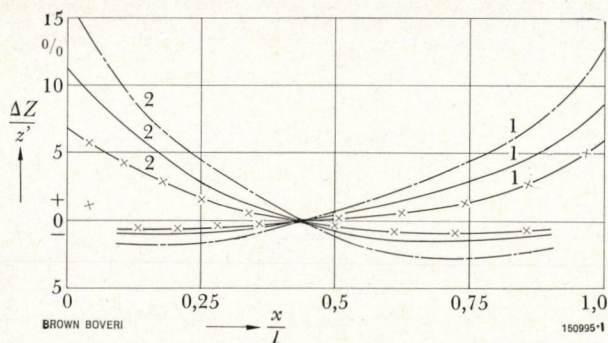


Fig. 5. — Error in measurement (ΔZ) of distance relays 1 and 2 (Fig. 4) under earth fault on a double-circuit line with supply at both ends. The error is expressed as a percentage of the relevant desired value $z' x$ (without compensation)

- 1 = Relay 1
- 2 = Relay 2
- + = Measured impedance too great
- = Measured impedance too small
- = $z^m = 0.7 z^0$
- = $z^m = 0.5 z^0$
- x-x- = $z^m = 0.3 z^0$
- l = Length of line
- x = Distance of fault from C
- z' = Direct or indirect impedance in the protected line

The ratio z^m/z^0 is normally between 0.4 and 0.6. The effect of the mutual zero impedance on the accuracy of measurement was calculated for a double-circuit line with equal supply at both ends and a third connection between C and D. The errors in measurement by relays 1 and 2 for all locations between $x = 0$ and 1 are shown in Fig. 5. The curves were determined for $z^m = 0.3 z^0$, $0.5 z^0$ and $0.7 z^0$. In these cases the error of relay 1 is between 2.5% (where $z^m = 0.3 z^0$) and 6% (where $z^m = 0.7 z^0$) for a single-phase fault at 85% of the line length. The error of relay 2 is between 3.8% ($z^m = 0.3 z^0$) and 8% ($z^m = 0.7 z^0$). Under normal circumstances where z^m is about $0.5 z^0$ the maximum error at the step limit (about 85% of line length) will not exceed 5.5%.

The error depends on the relative magnitude of the supply impedances, the fault resistances and the positions of the phase voltage vectors at bars C and D when the fault occurs [1].

Compensating the Error in Measurement; Other Remedial Measures

The following are some of the measures which can be applied to attain accurate distance measurement and/or rapid interruption of a single-phase earth fault along the protected line:

- a feeding the neutral current of the parallel line into the relay
- b switched compensation [2, 3] by the zero sequence current of the parallel line
- c correction by changing factor k_0 [4]
- d deliberately setting k_0 to a different value than necessary
- e interconnecting the relays at both ends of the line

With method a a fraction $\alpha = z^m/3 z'$ of the summation current $3 I_3^0$ of the healthy circuit (line 3-4 in Fig. 4) is fed to the relays of the faulted phase. Therefore the current governing the measurement is

$$I_1^R + k_0 \cdot 3 I_3^0 + \alpha 3 I_3^0$$

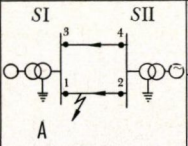
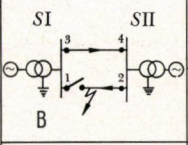
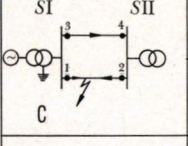
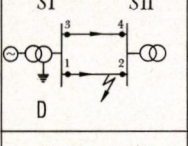
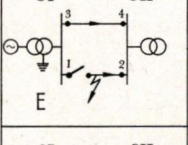
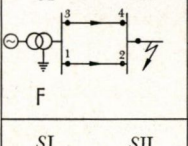
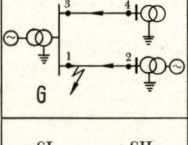
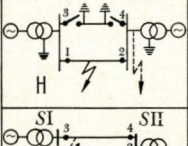
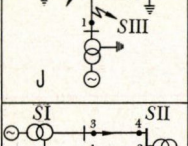
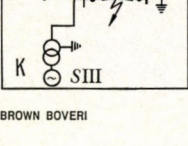
When this method is applied, the relay in the faulted circuit will measure correctly. To prevent a non-selective interruption of the sound line it is sometimes necessary for the summation current compensation to be effected from the sound line to the relay of the faulted line and not vice versa.

Where method b is used the compensating value is not connected before the ratio of the zero sequence current of the line considered to that of the other line is equal to or greater than unity.

With method c the correction factor k_0 of the relay is altered in relation to the magnitude and direction of the zero sequence currents in the line as follows:

- it is increased if the zero sequence current in the parallel line is in the same direction and equal to or less than the zero sequence current in the relay.
- it is reduced if the zero sequence current in the parallel line is in the opposite direction and equal to or less than the zero sequence current in the relay.
- it is reduced if the breaker in the parallel line is tripped by the appropriate relay.

The behaviour of distance relays under single-phase earth faults

		1				2				3				4			
		0	a	b	c	0	a	b	c	0	a	b	c	0	a	b	c
	M	→	+	+	-	→	+	+	-	→	→	→	-	→	→	→	-
	V	+	+	+	+	+	+	+	+	+	-	+	+	+	(+)	+	+
	M					→	+	+	-	→	→	→	-	→	→	→	-
	V					+	+	+	+	+	⁹⁹⁾ Δ (-)	⁹⁹⁾ Δ (-)	(+)	+	(-)	+	+
	M	→	+	+	-	→	+	+	-	→	→	→	-	→	→	→	-
	V	+	+	+	+	+	+	+	+	+	-	+	+	+	+	+	+
	M	→	+	+	-	→	+	+	-	→	→	→	-	→	→	→	-
	V	+	+	+	+	+	+	+	+	+	(+)	+	+	+	+	+	+
	M					→	+	+	-	→	→	→	-	→	→	→	-
	V					+	+	+	+	+	-	Δ	Δ	+	+	+	+
	M	→	+	+	-	→	+	+	-	→	+	+	-	→	+	+	-
	V	+	+	+	+	+	+	+	+	+	+	+	+	+	+	+	+
	M	→	+	+	-	→	+	+	-	→	→	→	-	→	→	→	-
	V	+	+	+	+	+	+	+	+	+	⁹⁹⁾ (-)	+	+	+	+	+	+
	M	→	→	→	-	→	→	→	-								
	V	+	+	+	+	+	+	+	+								
	M	→	→	→	-	→	→	→	-	→	→	→	-	→	→	→	-
	V	+	+	+	+	+	+	+	+	+	+	+	+	+	(-)	+	+
	M	→	+	+	-	→	+	+	-	→	→	→	-	→	→	→	-
	V	(+)	+	+	+	+	+	+	+	+	⁹⁹⁾ Δ	⁹⁹⁾ Δ	(-)	+	+	+	+

BROWN BOVERI

160996-1

- ◀ 1, 2, 3, 4 = Relays
 0 = Without compensation
a, b, c = Method of compensation
 A to K = Switching arrangements
M = Measurement by distance relay
 SI, SII, SIII = Substations
V = Behaviour of distance relay (tripping)
 + = Correct measurement (tripping or blocking)
 - = Incorrect measurement (tripping or blocking which can endanger the distance step grading)
 () = Probable response
 |→ = Relay overreaches (opposing zero sequence currents)
 |← = Relay underreaches (parallel zero sequence currents)
 * = Correct operation with separate directional element without compensation
 ** = Selectivity is possible because of intermediate supply at station II
 *** = Compensation impossible
 Δ = Distance step grading endangered because only relay 2 has compensating current and relay 3 overreaches due to lack of compensating current

- it is reduced if the parallel line is interrupted and earthed at both ends (possibly by manual switching).

This method does not provide accurate distance measurement but ensures correct behaviour of the relay.

With method *d* the coefficient k_0 is set somewhat higher than would be necessary for the line without considering the mutual impedance so that the error in measurement can be partly compensated.

Method *e* involves an auxiliary link such as RF signal transmission, microwave equipment or a pilot connection [5] but provides selective and rapid interruption under all switching arrangements and supply conditions.

Comparing the Various Methods of Compensation and Their Operation

The behaviour of the distance relays under single-phase earth-fault conditions and using methods *a*, *b* and *c* for various switching conditions on a double-circuit line are shown in the Table. The interruptions are assumed to be three-phase.

Cases A and B with Supply at Both Ends

The distance measurement of relays 1 and 2 on the faulted line is affected if no compensation is used. An earth fault at the beginning of the line causes a three-phase interruption at both ends of the line in cascade because the second relay trips immediately after the first without waiting for the time-lag of the second step to elapse [6]. If an RF link (permissive underreach transfer tripping or carrier acceleration [5]) is used, interruption of breakers 1 and 2 is almost simultaneous.

The relays in the sound line, which possibly measure smaller impedances because the zero sequence currents in the two lines are in opposite directions, do not trip because of their directional characteristics.

If compensation by method *a* is used, the distance relays of the faulted line measure correctly, and those of the sound line wrongly because they cannot be compensated with the correct current. It is therefore possible for the sound phase to be interrupted for no real reason. If a separate directional element is used which is not compensated by the zero sequence current of the other line, this incorrect interruption is prevented. On the other hand there are the well known complications involving racing between the directional and measuring elements. After breaker 1 has opened, relay 3 of the sound line would overreach due to lack of compensating current so that the selectivity with respect to relay 2 at the other station would be jeopardized, especially if this is correctly compensated and trips in the second step.

Methods *b* and *c* do not have the first drawback because the quantities (e.g. zero sequence current in the sound line) which upset the selectivity are not fed to the relay. The possibility of non-selective operation between relays 2 and 3 after breaker 1 opens is not, however, overcome by using these methods.

Cases C, D and E with Supply at One End

Uncompensated relays on the faulted line behave in the same fashion as in cases A and B. The relay at the supply end of the sound line underreaches. At most this can lead to a delay in the back-up steps. Although it has a tendency to overreach the relay in

the opposite station will not trip because of the directional characteristics of the measuring elements.

Method *a* once again leads to a false distance measurement on the sound line. Selectivity between relay 3 at the supply end and relay 2 at the opposite station is disrupted. If the fault is in the first half of the line viewed from the supply end, both relays can trip simultaneously.

Methods *b* and *c* enable correct behaviour of the relay (or the required selectivity) to be attained but without eliminating the second drawback (cf. cases A and B). On the other hand a carrier connection between the relays at both ends of the protected line (method *e*) would ensure rapid and selective interruption of all faults on this section.

Case F with External Fault

Without compensation both of the relays at the supply end underreach. For this reason there is no danger to the distance-time step grading and the only possible effect would be a lag in response in the back-up stage which is also easily possible as a result of intermediate supply at station II.

Switched compensation should become effective when the summation currents in both lines are equal. In this case also the interruption would be rapid and selective when using method *e*.

Case G with Parallel Lines Separated at One End

Apart from one aspect the uncompensated relays behave similarly to case A. As the zero sequence currents in the two parallel lines are directionally opposed to each other at the connected end, relay 1 at the supply end will overreach and it is therefore theoretically possible for this relay to interfere with the distance-time steps of the other relays if there is no infeed from station II. In practice, however, this error is so small that selectivity is not affected.

Compensation by method *a* could lead to a non selective interruption of the sound line.

With switchable compensation by methods *b* and *c* the relays behave properly. In this case also method *e* attains the requisite selectivity.

Case H with the Parallel Line Interrupted and Earthed

The relays without compensation overreach and there is a possible danger to the distance step grading. On the other hand it is not possible to use methods *a* or *b* because no current is flowing in the current transformers connected to the parallel line. On the other hand with method *c* it is possible to make a correction to factor k_0 with suitable logic circuits so that the relays measure properly. Selecting a suitable method of coupling (method *e*) enables selective and rapid interruption of the fault to be attained.

Cases J and K

If a fault occurs in the vicinity of stations III or I, relay 2 in station II overreaches and this can disrupt the distance-time step grading. Relay 3 also overreaches and if there is no supply at station II there is also a possibility of danger to the distance-time step grading. Proper compensation can be provided only for relays 2 and 4. Compensation by methods *a*, *b* or *c* for relays 1 and 3 (this is possible in case K only) leads to false distance measurement and also non-selective tripping. Method *e*, however, retains the selectivity.

Although method *c* is theoretically feasible it involves a great deal of complicated equipment. It is no simple matter to calculate the modifications to correction factor k_0 and in certain cases it can lead to considerable corrections. The result of this is high capital outlay and/or a large CT burden.

Method *d* is a very much simplified version of method *c* and can naturally not work satisfactorily in every case.

Summarizing it can be seen from the Table and the above considerations that although compensating the mutual effect of the zero sequence current circuit leads to an improvement in the distance measurement by the relays connected to the faulted line the selectivity of the relays on the sound line can be endangered under certain operating conditions.

There are also cases where it is impossible to compensate. If, for instance, we change from case C to case K, the compensation in K would have to be rendered ineffective to prevent any non-selective tripping and to ensure that station II does not become isolated.

Apart from method *e* the methods mentioned are all designed for relays with a single system of measurement where only the sound phase is measured. In cases where relays employing several systems of measuring elements are used, the relays connected to the sound phases could trip erroneously during single-phase earth faults due to the additional compensation current if methods *a*, *b*, *c* or *d* are used. Fundamentally the same considerations apply to single-phase reclosure if we ignore insignificant exceptions.

Conclusions

Errors in measurement by distance relays occur during earth faults on double-circuit lines because of the mutual effects of the zero sequence systems in the two lines. It is fundamentally possible to avoid these errors with respect to the faulted line by suitable compensation. Under certain operating conditions, however, it is not possible to apply compensation because it would disturb the selectivity of the sound line.

It is possible, on the other hand, to use suitable methods of coupling between the relays at both ends

of the protected line, such as permissive underreach transfer tripping or carrier acceleration [5] and interrupt an earth fault selectively and with no delay on a double-circuit line without using any special compensation systems.

(AH)

H. UNGRAD
V. NARAYAN

Bibliography

- [1] C. ADAMSON: Error of sound-phase compensation and residual compensation systems in earth-fault distance relaying. *Proc. Instn elect. Engrs* 1965, Vol. 112, No. 7, p. 1369-82.
- [2] V. KADNER, G. WACARDA: Verhalten von Distanzrelais in starr geerdeten Netzen. *Energietechnik* 1958, Vol. 8, No. 12, p. 569.
- [3] O. POSSNER, G. WACARDA: La protection de lignes doubles et multiples. CIGRE Report No. 327, 1962.
- [4] H. UNGRAD: Probleme bei der Disposition statischer Schutzrelais. Thesis, TH Vienna, 1966.
- [5] J. GANTNER: Brown Boveri distance protection systems employing carrier transfer. *Brown Boveri Rev.* 1968, Vol. 55, No. 7, p. 365-71.
- [6] A. MATTHEY-DORET: Line and cable protection, the main features and application. *Brown Boveri Rev.* 1966, Vol. 53, No. 11/12, p. 834-40.

Thyribloc—A New Range of Liquid-Cooled Thyristor Converters

621.314.58:621.382.233-713

The steadily decreasing cost of thyristors is continuously opening up new opportunities for controlled semiconductor converters. New production methods in the chemical and other industries, for example, are becoming economically attractive. More highly rationalized manufacture and improved quality of the end product, or increased utilization of plant, are grounds for using thyristors in the power supply, particularly in the field of electrochemistry, even though thyristors are still more expensive than diodes.

The Thyribloc range of liquid-cooled SCR converters has been developed to supplement the Thysert and Thyristack ranges, which have natural or forced air cooling. This construction and possible applications of this new type of converter are reviewed in this article.

Introduction

Hitherto we have been able to offer converter installations employing thyristors with natural or forced air cooling, under the names "Thysert" and "Thyristack" [1, 2]. In cases where the ambient air is corrosive or heavily polluted, or the air requirement is very large, it may be necessary to fit a very expensive fresh-air filter or use mixed or closed-circuit air cooling. This has an important influence on the layout and cost of the installation [3]. Therefore, if there is no other equipment which needs a closed-circuit air system, direct liquid cooling of the converter devices offers great advantages. Experience has confirmed this in the case of heavy-current equipment for large electrolyzers.

Liquid cooling makes for compactness [4], which is desirable with heavy-current plant because the available space is better utilized, voltage drops are smaller and the material and installation costs of

the busbars are lower. In heavy-current installations the cost of materials for separate busbars and heat sinks represent a comparatively large proportion of the total cost of the converter. A heavy-current converter of economical design must therefore employ a low-priced material for the busbars, and if possible a combination of bars and heat sinks. These points were considered some years ago in conjunction with heavy-current diode rectifiers, and led to the "Rectibloc" range of rectifiers [5], which make wide use of aluminium. This design has proved itself in practice (rectifier installations of this type for a total of 2500 kA are in service), and it was therefore logical to employ the same design principles for heavy-current installations incorporating thyristors.

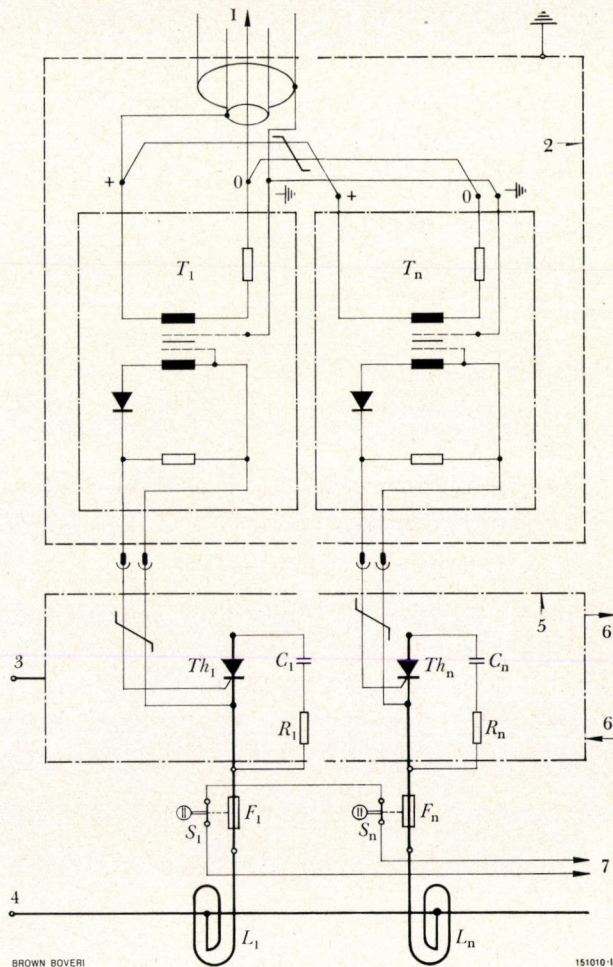
The Thyribloc Range

The Thyribloc range complements the Thysert range and, because the equipment is liquid-cooled, opens the way to new applications and new arrangements. Intended for heavy-current low-voltage installations, Thyribloc units are specially designed for corrosive atmospheres.

Field experience with thyristor converters has shown that faults in the semiconductors are rare. The failure rate for thyristors is of the same order as for diodes. If a converter is designed for $n-1$ service, this means that, if one thyristor should fail in each limb of the circuit, the installation can still be operated continuously at rated capacity. Availability is then not affected in the case of converters which

Fig. 1. - Circuit diagram of a converter limb

1 = Pulse wiring to control set
 2 = Screen
 3, 4 = Main supply terminals
 5 = Combined heat sink and busbar of extruded hollow-section aluminium
 6 = Coolant inlet and outlet
 7 = Component fault indication
 T_1-T_n = Pulse transformers
 Th_1-Th_n = Thyristors
 $R_1C_1-R_nC_n$ = RC networks
 F_1-F_n = Fuses
 S_1-S_n = Indicator switches
 L_1-L_n = Air-core reactors
 Indices 1 to n indicate the parallel units for each heat sink.



are normally switched off every few days or can occasionally be taken out of service. Any faulty components can be changed the next time the converter is shut down, and there is thus no need to provide facilities for in-service replacement of parts.

Electrical Design

The circuit of one limb of a Thyribloc converter is shown in Fig. 1. The basic circuit diagram of a complete Thyribloc in three-phase double-star anti-parallel connection can be seen in Fig. 2.

The questions of specifying and dimensioning the various components will not be discussed here, as they have already been dealt with in an earlier article [6]. Overvoltages caused by sudden collapse

of the reverse current (the hole-storage effect) are damped by RC networks connected in parallel with each thyristor. In series with each thyristor is an air-core reactor L which reduces the turn-on current and the rate of rise of the forward voltage and improves the current distribution. Their effect on the current distribution is reinforced by the fact that they are wound in opposite directions and magnetically coupled with the neighbouring reactor. Turn-on losses in the first thyristor to fire in each limb are limited by a resistor R in the surge-damping circuit and air-core reactors L . Resistor R has the further task of reducing oscillations on commutation to an acceptable level.

The characteristic of fuses F (Fig. 1), which are in series with the thyristors, were not matched to the

limit-current characteristics of the thyristors, for the following reasons:

- In heavy-current installations operating at constant load, losses are assessed at as much as SFr. 2000 per kW. Losses due to the fuses must therefore be as low as possible.
- In heavy-current low-voltage installations, the likelihood of a dead short circuit on the d.c. side is negligible, and the effect of the secondary-side busbar connections on the magnitude of the short-circuit current is so great [7, 8] that it is most unlikely that the thyristors will be stressed beyond their overcurrent capability during the opening time of the primary breaker, or d.c. breaker if there is one.

Faults are monitored by an auxiliary fuse element which is integrated with the main fuse. It is acceptable to use auxiliary elements for fault detection in conjunction with unmatched fuses because the ele-

ments respond to the reverse current in the event of an internal short circuit. A switch S (Fig. 1) which gives visual indication of a fault is actuated mechanically if the auxiliary fuse element melts. All normally-closed contacts of these switches are connected in series in each limb of the converter and, depending on the size of the converter, can be used to indicate faulty components and to disconnect the equipment.

The trigger circuit, with special pulse transformers T (Fig. 1), is electrically identical to that in the Thysert range [1]. Effective geographical separation of the control circuits from the power circuits was found to be impracticable. By employing a specially designed screen 2 (Fig. 1) of grain-oriented sheet, locating the pulse transformers in a favourable position, and providing certain earthing facilities, however, it has been possible to reduce inductively and capacitively-borne interference to a power level which is far below the firing power of the thyristors. To test these screening measures, steep-fronted pulses

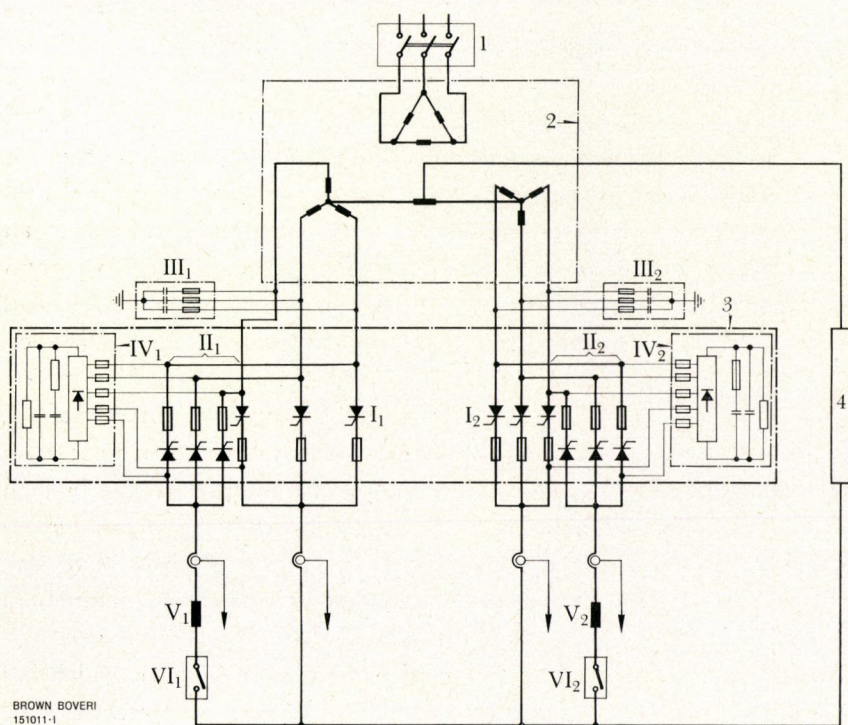


Fig. 2. - Circuit diagram of a supply system in double three-phase star anti-parallel connection

- 1 = Circuit-breaker
- 2 = Transformer
- 3 = Thyristor
- 4 = Load
- I_1, I_2 = Double three-phase star connection for forward current at load
- II_1, II_2 = Double three-phase star connection for reverse current at load
- III_1, III_2 = Transformer protection against overvoltages transferred capacitively from primary side
- IV_1, IV_2 = Decoupled capacitor providing protection against overvoltages on a.c. and d.c. sides
- V_1, V_2 = Reactor to damp circulating currents
- VI_1, VI_2 = D.C. circuit-breaker

with a rate of rise of $8 \cdot 10^7$ A/s were applied to the heat sinks 5 carrying the pulse transformers. The tests confirmed their effectiveness in preventing the power side from interfering with the control circuits.

Every Thyribloc includes protection against switching overvoltages. It consists of a capacitor which is able to absorb the magnetic energy of the converter transformer without the voltage exceeding transient maximum peak voltage of the thyristors. The capacitor is connected via decoupling diodes to the transformer secondary side and the d.c. side, and thus damps any overvoltages occurring on the a.c. and d.c. sides.

Construction

The Thyribloc, like the Rectibloc [5], is built up from extruded aluminium sections. Certain aluminium alloys have performed extremely well in many rectifier installations exposed to corrosive atmospheres. This is true both of the high corrosion resistance to air containing salt or chlorine, and also of the junctions with copper parts. Suitable contact surface treatment has completely eliminated this latter problem.

Versions mounted in an open frame and in an air and dust-tight cabinet are available to meet different site conditions. The construction of the converter itself is the same in both instances.

The thyristors are mounted on hollow-section extruded aluminium which serves both as a conductor and as a heat sink. The lower end of this heat sink has a hose union appropriate to the coolant used, while at the top there is a double elbow to divert the coolant down again. Return of the coolant to the inlet point results in a uniform temperature level over the entire height of the heat sink.

The flat-base thyristors are clamped to the heat sink by means of a spring retaining plate. The problems of establishing contact between the heat sink and thyristor, due to the double function of the fixing as both thermal and electrical conductor, have been solved in the same way as with the Rectibloc [5].

The air-core reactors for each thyristor are welded by one end to a busbar running parallel to each heat sink. The fuses are at the other end of each reactor.

An aluminium alloy with good electrical conductivity and adequate mechanical strength is used for these reactors. Instead of the inter-turn insulation used in the past, the aluminium sections receive an oxide skin 50 μm thick before being worked. The aluminium oxide provides sufficient insulation together with efficient heat removal. Each reactor is clamped individually and relative to the neighbouring reactors by means of glass-fibre insulation and fixing bolts so as to absorb the electrodynamic forces caused by an internal short circuit. The reactors are alternately wound in opposite senses and arranged so that the busbar passes through their centres.

The RC networks for the hole-storage effect are immediately next to the thyristors. The pulse transformers for firing the thyristors are also close by the thyristors. These transformers are surrounded by magnetic screening.

Thyriblocs can generally be adapted to suit the position required, e.g. free-standing or wall-mounted. Because of the construction, the busbar connections for a.c. and d.c. can be brought out only at top and bottom. The maximum current permissible for each converter unit is then 30 kA with double three-phase star connection. However, any current can be handled by connecting a number of units in parallel.

Cooling System

Power dissipated by the thyristors is removed via heat sinks by the coolant which flows in closed-circuit cooler groups. These groups can be suited to local conditions and other special requirements.

Where there is a sufficient supply of water, whether from the public supply, a cooling tower, a river or the sea, this is the ideal primary coolant. If there is a shortage of water, outside air may be used. On the secondary (converter) side the coolant can be transformer oil, chlorinated diphenyls or deionized water. If transformer oil is used, the maximum temperature of the primary coolant should not exceed 35 °C, while for temperatures up to 45 °C the only possible coolant on the converter side is water.

The most common Thyribloc arrangements

Connection and enclosure	Range of rated d.c. current per Thyribloc unit kA	Arrangement	
		Plan	Section
3-phase star connection on one heat sink	2 to 9		
3-phase midpoint connection on 3 heat sinks, in 1 cubicle	5 to 15		
3-phase bridge connection in 1 cubicle	2.5 to 7.5		
3-phase bridge connection in 2 cubicles	5 to 15		
Double 3-phase star connection in 2 cubicles	10 to 30		
3-phase bridge connection (antiparallel) in 2 cubicles	2 x 5 to 15		
Double 3-phase star anti-parallel connection	2 x 10 to 30		

1 = Heat sink of extruded hollow section aluminium
 2 = Aluminium busbar
 3 = Air-core reactor

4 = Fuse
 5 = Thyristors

By establishing these maximum values on the basis of a minimum temperature difference of 10 deg C, it is possible to obtain the optimum arrangement of the cooler group with respect to cost and size.

The cooler groups can be installed wherever is most convenient. They can, for example, be situated directly by the converter cubicle in the open version, or mounted in an enclosure to harmonize with the cubicle. They can be installed separate from the converter in a neighbouring room or on a lower floor. These solutions are particularly well suited to liquid cooling, as connections to a water supply are usually to be found nearby. If air is used for cooling, the best place is outside the building, e.g. in a shaded yard or on a roof exposed to the wind.

Cooling the converter with transformer oil involves the least expense as regards the cooler group. The group then consists of the heat exchanger, a glandless circulating pump, an expansion vessel, the pressure and temperature monitoring instruments, stop valves and connections for supplying the coolant to the converter. Since the insulating capacity of the oil decreases only very slightly during service, and the oil temperature anyway reaches 55 °C only in exceptional cases, maintenance of the secondary side of the cooling circuit presents no problems. One must assume, however, that the primary side will need to be inspected more frequently than the secondary. This will depend of the purity of the coolant.

The cost is higher if deionized water, instead of transformer oil, is used as the secondary coolant. To ensure that the specific resistance of the water remains above the minimum value of 20000 Ωcm , an ion exchanger has to be installed in a shunt circuit. The two-stage ion exchanger used has the advantage that it can be regenerated without having to remove it from the equipment. To allow ordinary steel and cast iron to be used for the cooling circuit, a corrosion inhibitor is added to the water. The system is also carefully sealed to exclude any oxygen. Normal tap water is suitable for installations with d.c. voltages up to 50 V, providing the specific resistance of the water is about 2000 Ωcm . A recirculating system is then not necessary. However, it is advisable to provide means of softening the water.

The Different Versions and Applications

As mentioned at the beginning, the Thyribloc is intended to supplement the Thysert. Its design is such that the most economical range of application lies between ratings of 5 and 30 kA per converter unit. The economic limit of a liquid-cooled Thyribloc, as opposed to the air-cooled types, can, however, extend below 5 kA if the converter is to be located in a corrosive atmosphere, in which case it must be totally enclosed and an air/water recooling system is therefore required.

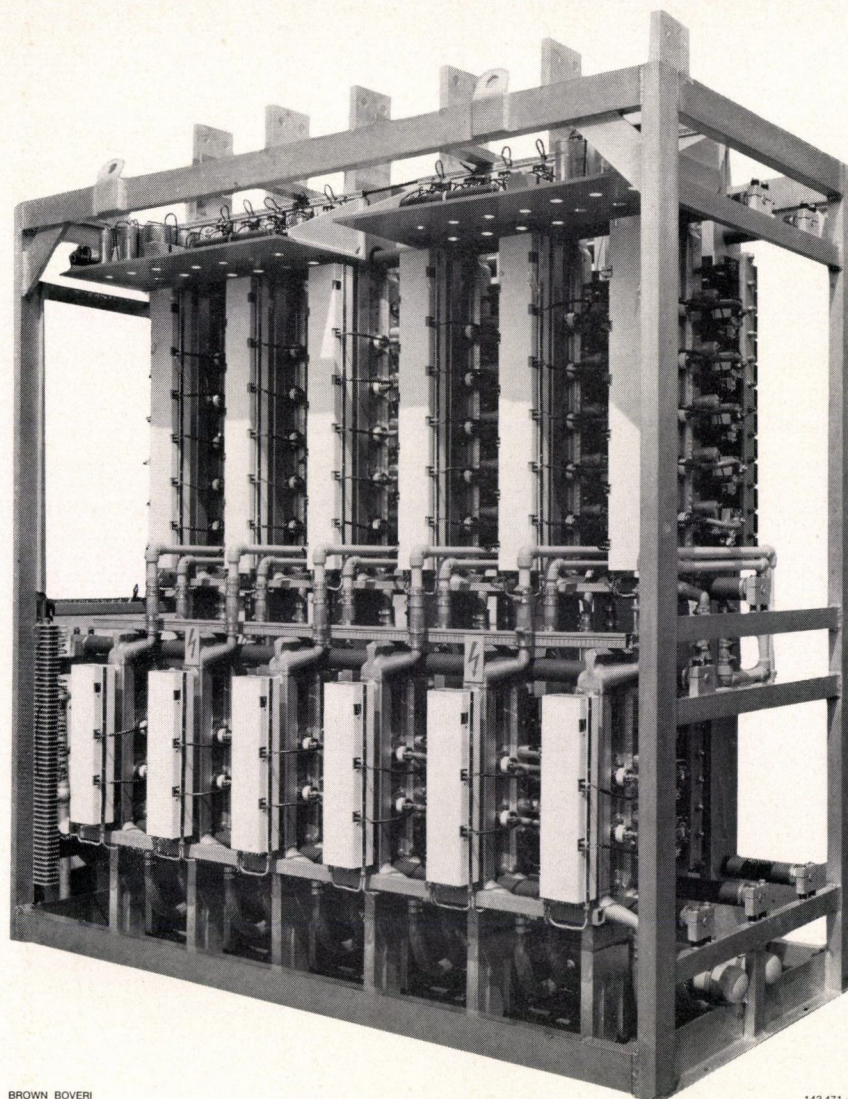
It can be seen from the Table that with Thyriblocs virtually any normal converter circuit arrangement, either for drives [9] or for electrochemical and other heavy-current d.c. applications, can be contained in a single or double rack, or alternatively in a cubicle.

With the Thyribloc range it is not possible to connect thyristors directly in series. If the d.c. voltage is comparatively high, complete converter units are series-connected. In view of the steadily increasing voltage ratings of power thyristors, it will soon be possible to produce practically any service voltage required for heavy-current installations, without having to connect either thyristors or entire converter units in series.

The number of thyristors to be connected in parallel has to be determined for each particular case, since it is governed by the service current of the thyristors and the facilities for cooling.

Thyristor-controlled heavy-current installations with liquid cooling generally provide an economical solution wherever rapid response is required, such as for electrolyzers with current reversal, coils for agitators, magnet supply systems and power network interties. The favourable trend in the price of low-blocking thyristors indicates that the controlled rectifier will in the near future find more new applications in low-voltage installations up to about 50 V, such as electrolyzers and galvanic plating plant. The Thyribloc design is particularly suitable for these applications.

In conclusion, it should be mentioned that the Thyribloc converter shown in Fig. 3 has been operating faultlessly for about a year in the electrochemical industry. The main data of the installation are:



BROWN BOVERI

143 471 - I

Fig. 3. — Thyribloc in open frame, for double three-phase star antiparallel connection

Current rating in forward direction $I_{d1_1} = 15\,000\text{ A}$
 Current rating in reverse direction $I_{d1_2} = 7\,500\text{ A}$
 No-load d.c. voltage $U_{d1_0} = 180\text{ V}$
 Double three-phase star antiparallel connection

of the reverse current, because its r.m.s. value is only approximately 4 kA.

(DJS)

E. KELLER
M. QUISSEK

Although the converter is in antiparallel connection, and free from circulating currents, the customary protection against circulating currents, comprising an air-core reactor and a d.c. circuit-breaker, has not been omitted. The d.c. breakers and current-limiting reactors are in this case located in the path

Bibliography

- [1] H. PISECKER, X. VOGEL: "Thysert", a new element of the Brown Boveri electronic system. Brown Boveri Rev. 1967, Vol. 54, No. 5/6, p. 241-50.
- [2] P. SCHNEIDER: Rectistack and Thyristack converters as power elements of the Brown Boveri electronic system. Brown Boveri Rev. 1965, Vol. 52, No. 4, p. 310-17.

- [3] W. BERLE: Ventilation techniques for industrial installations. Brown Boveri Rev. 1964, Vol. 51, No. 7, p. 452-8.
- [4] H. J. BOSSI: Planning rectifier installations. Brown Boveri Rev. 1966, Vol. 53, No. 10, p. 636-45.
- [5] E. KELLER: The "Rectibloc" silicon rectifier. Brown Boveri Rev. 1965, Vol. 52, No. 4, p. 318-23.
- [6] G. IRMINGER: Thyristor circuitry. Brown Boveri Rev. 1966, No. 10, p. 657-71.
- [7] W. KLEINMANN, G. REICHE: Gleichstromanspeisung von Elektrolyseanlagen. BBC-Nachr. 1964, Vol. 46, No. 6/7, p. 325-32.
- [8] H. WIDMER: Entwurf und Betrieb grosser Gleichrichteranlagen. Bull. schweiz. elektrotech. Ver. 1965, Vol. 56, No. 15, p. 597-602.
- [9] H. PISECKER: Semiconductor converters for electric drives. Brown Boveri Rev. 1966, Vol. 53, No. 10, p. 672-87.

High-Voltage Rectifiers for Large Transmitters

621.314.6.027.6/7:621.396.61

As transmitters become larger, the requirements to be met by the supply rectifiers are becoming more exacting. Even now, anode voltages up to 20 kV and anode currents up to 200 A are needed. The advantages and drawbacks of rectifiers employing thyratrons, thyristors or diodes are reviewed. The three-phase bridge connection customary for transmitter rectifiers and sizing of the filters are discussed. Different protection systems for rectifiers incorporating diodes are then compared.

proved, however, an increasing proportion of transmitters obtain their power via thyristors or diodes. Since both types of rectifier system, whether employing tubes or semiconductors, are now contenders for use in large transmitters, they are discussed below, together with their advantages and disadvantages.

Introduction

Transmitters with outputs of up to some 1000 kW require anode voltages up to 20 kV and anode currents up to 200 A. Rectifier development has kept pace with the ever more exacting demands. Because of their low efficiency, the high-vacuum hot-cathode tube used in the early days of transmitters were soon replaced by mercury-arc rectifiers. These became known as mutators and evolved comparatively quickly from uncontrolled devices to controlled, six-phase units. The rectifier tanks were improved at the same time. At first the high vacuum had to be constantly maintained by means of pumps, but later it became possible to produce sealed tanks. Unfortunately, these had the disadvantage that, if an anode or a grid failed, the whole unit had to be replaced.

The introduction of gas-filled, single-anode rectifier tubes thus represented an important advance, and these have been in service for many years in a large number of installations. As semiconductors are im-

Rectifiers with Tubes

Rectifier tubes include ignitrons, excitrons and thyratrons. These single-anode devices have the advantage over mercury-arc rectifiers that they can be combined to form any circuit arrangement, and are easily replaced. Ignitrons and excitrons have mercury-pool cathodes. The ignitron is triggered with an ignitor, while with the excitron an arc has to be maintained continuously by the ignition and excitation system associated with each tube. Ignitrons are more suitable for small voltages and large currents. They are therefore rarely used in rectifiers for large transmitters. Moreover, the ignitor requires a much higher driving power than the control grid of an excitron or a thyatron. The life of excitrons and ignitrons is shortened if they are operated for long periods at voltages reduced by grid control because, as with mercury-arc types, the internal insulation accumulates deposits.

For these reasons thyratrons with hot cathodes have become widely used. Each tube, of course, has to be heated and controlled. With the three-phase

bridge arrangement described in the following section the filament power can be fed jointly to the top three tubes. On the other hand, separate leads for the filament power have to be provided for the bottom three tubes, as the cathodes of these are connected to the alternating-voltage potentials of the high-voltage transformer. The same applies to the control leads to all six tubes. This apparent drawback is no longer of any significance, now that transformers of low power and high insulation rating can easily be manufactured with the aid of synthetic resins.

Figures 1 and 2 illustrate the rectifier for a 1000 kW transmitter. Rated 15 kV and 200 A, the rectifier is equipped with Brown Boveri thyratrons type TQ101. The heating and control transformers for each tube can be seen in Fig. 2. These are of the moulded resin type and designed for a test voltage of 45 kV a.c. The control circuit is fully earthed. In this particular installation the control transformers

have special supersaturated cores, thus providing a simple way of generating needle-shaped pulses for the control grids.

The Three-Phase Bridge

The three-phase bridge circuit commonly used for transmitter rectifiers is shown in Fig. 3. For the same d.c. output voltage, the reverse voltage per tube is here only half as high as with the six-phase connection customary with mercury-arc equipment and the tubes conduct for 120° el, and not 60° el. Utilization is thus greater, and the transformer can be made simpler and with a rating some 30% lower than needed for a six-phase arrangement. Half the service voltage is present at the transformer neutral, although hum is greater than with the circuit usually employed for mercury-arc tubes.

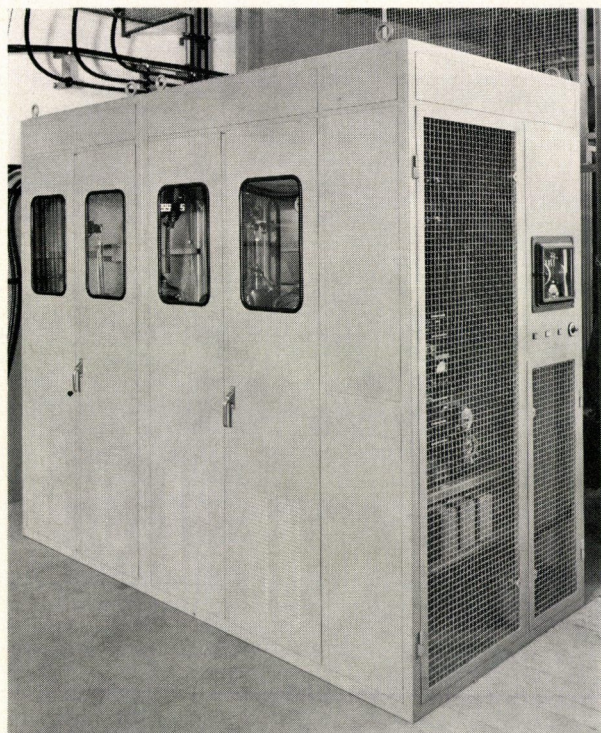


Fig. 1. — High-voltage rectifier for 15 kV and 200 A, employing thyratrons

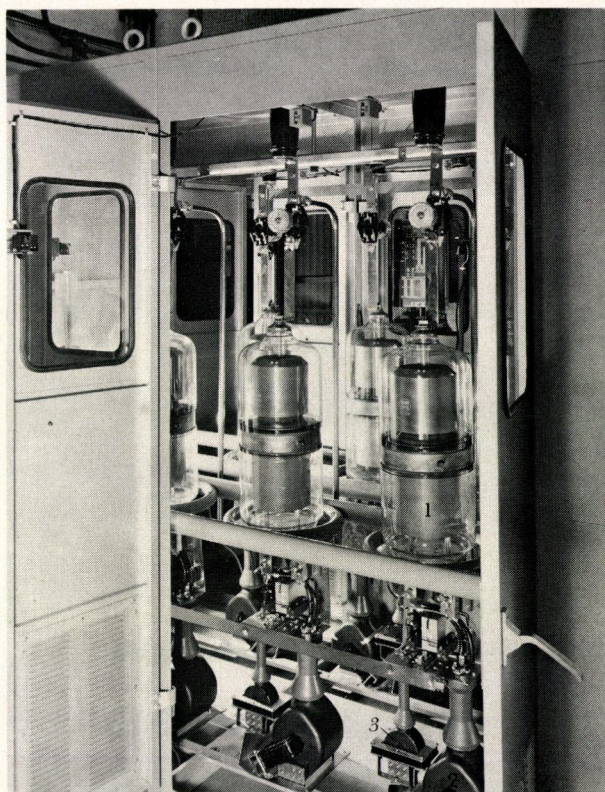


Fig. 2. — Inside the high-voltage rectifier of Fig. 1

- 1 = Brown Boveri thyatron type TQ 101
- 2 = Heating transformers
- 3 = Control transformers

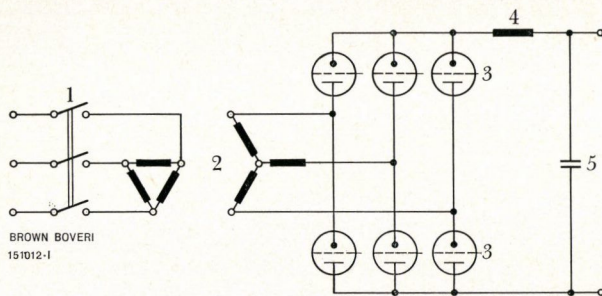


Fig. 3. - Three-phase bridge connection

- 1 = Circuit-breaker
- 2 = Transformer
- 3 = Controlled thyratrons
- 4 = Filter choke
- 5 = Filter capacitance

In a three-phase bridge, one upper and one lower tube must always be conducting, as otherwise the circuit is not closed. It can thus be considered as two three-phase rectifiers connected in series. This is apparent from the curves of voltage shown in oscillogram a_1 of Fig. 4. Oscillogram a_2 shows the summation voltage of the upper and lower curves.

In b_1 the firing angle has been delayed by 20° , resulting in corresponding discontinuities in the voltage curves. This is shown clearly by the curve of summation voltage in b_2 . Oscillograms c_1 and c_2 show the same when the firing angle is advanced by 45° , and the d.c. output voltage \bar{U} is correspondingly lower.

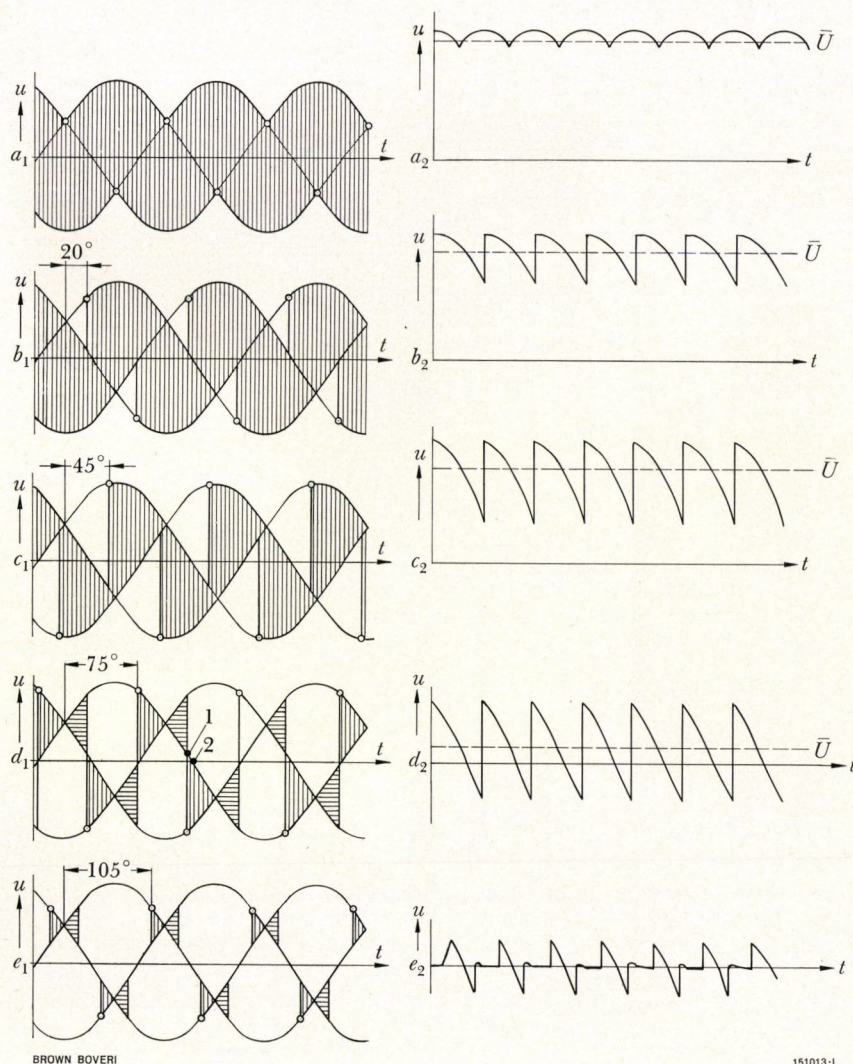


Fig. 4. - Voltage oscillograms for a three-phase bridge connection

a_1, b_1, c_1, d_1, e_1 :

Oscillograms for thyra-trons at different firing angles, i.e. different voltage levels

- ▨ = Positive output voltage
- ▩ = Negative output voltage

a_2, b_2, c_2, d_2, e_2 :

Summation voltages supplied by rectifier at different firing angles

- \bar{U} = Mean d.c. voltage output
- 1 = Firing point of an upper tube
- 2 = Voltage zero of a lower tube

If the firing angle is shifted by 75° (Fig. 4 d₁), negative summation voltage occurs, as shown by oscillogram d₂. Up to a certain firing angle, however, the current continues to flow without interruption because during the positive periods the filter choke is charged sufficiently to bridge the negative periods.

Oscillogram e₂ shows that when the firing angle is shifted by 105° (Fig. 4 e₁), actual gaps in the flow of current occur because the choke charged up during a positive interval can at most bridge only a negative interval of the same length (the areas of the positive and negative portions are approximately equal). The voltage remains zero during the periods of non-conduction, and because of its symmetry the resultant summation voltage is also zero.

As mentioned earlier, with a three-phase bridge one upper and one lower tube always conduct simultaneously, and the control pulses are distributed accordingly. This presents certain problems each time the voltage is first increased to its full value. After the short control pulse a tube continues to conduct only if the circuit is closed across a tube on the opposite side. If a lower tube is triggered when none on the upper side is conducting, there is no complete circuit. The situation is the same if the order is reversed. An improvement is gained by inserting a resistor between the transformer neutral and earth. If the firing angle is shifted so that the lower half of the rectifier still has positive voltage for at least 60° el, it conducts until the next upper tube fires (see point 1, Fig. 4 d₁), and the circuit remains closed throughout the rectifier. The lower half ceases to conduct at point 2 of the same diagram. If the firing angle is further, as in Fig. 4 e₁ for example, continuous operation would no longer be possible. Consequently, the voltage cannot be increased from zero upwards. Double control pulses or a so-called midpoint filter are needed for this. In the first instance, each control pulse is repeated after an interval of 60° . In this way, each time a tube fires, a pulse goes to a tube on the other side so that current can flow as soon as a positive summation voltage exists across the bridge.

A midpoint filter is the term used for a circuit in which the transformer neutral is connected to earth not across a resistor, but across a series-connected inductance and capacitor. This has the effect of

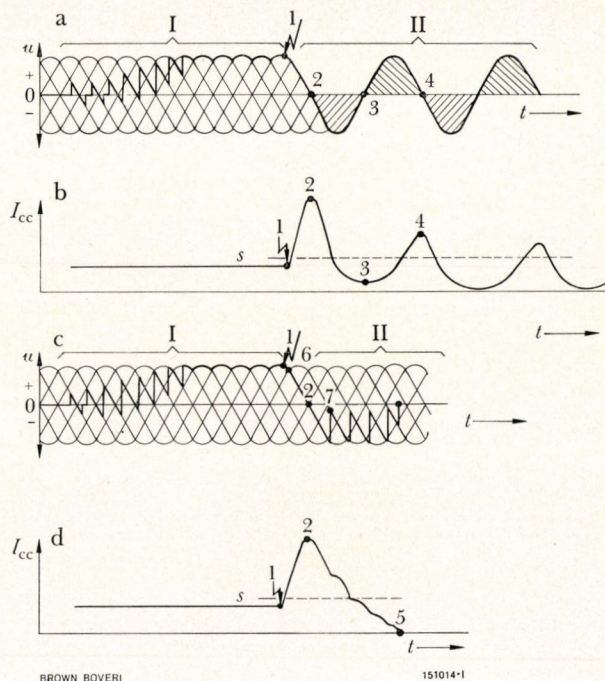


Fig. 5. - Oscillograms illustrating grid control

- a: Progressive increase of voltage (interval I) and interruption of short circuit without recuperative control (interval II)
- b: Current oscillogram for a
- c: Progressive increase of voltage (interval I) and interruption of short circuit with recuperative control (interval II)
- d: Current oscillogram for c

I_{cc} = Short-circuit current
 s = Saturation limit of choke

Points 1 to 7 are explained in the text.

roughly doubling the length of the current pulses so that the voltage can be increased, starting from zero. Through utilizing the half of the voltage present at the transformer neutral, the desired control characteristic can be attained, without any further assistance, by means of the filter element which is in any case essential. On the basis of the processes shown in Fig. 4, section I of Fig. 5 illustrates how the voltage can be raised continuously from zero with the aid of the grid control system. The voltage can, of course, also be held at any intermediate value. This is particularly desirable for changing wavelengths in the case of short-wave transmitters.

The principal advantage of grid control lies in dealing with short circuits, as in section II of Fig. 5. If a short circuit occurs at moment 1, for example, in the simplest case subsequent grid ignition will be suppressed. The anode which has just fired continues to burn, and passes through zero at 2 after approximately a quarter of a cycle. The short-circuit current can thus built up for a period of 5 ms at the moment, after which it is reduced again because the driving voltage passes into the negative region. The remainder of the interruption process is governed chiefly by the smoothing choke. If this is comparatively large, a correspondingly large amount of magnetic energy becomes stored as the short circuit is building up. The maximum short-circuit current I_{cc} at point 2 in Fig. 5 runs counter to the negative voltage in the negative half-cycle, and is reduced accordingly. It is possible, however, that this process is not complete by the time point 3 is reached. This is indicated by the fact that I_{cc} has not dropped to zero. The tube then continues to conduct during the next positive half-cycle, and the choke is once more charged up to point 4. This sequence can be repeated for a number of cycles, until current I_{cc} attains zero as a result of the ohmic resistances.

This undesirable situation can be remedied with the grid control in that the control pulses are not disconnected the moment a short circuit occurs, but are simply shifted in phase (so-called recuperation). Ignition of the next phase, which under fault-free conditions would take place at point 6, is then shifted to point 7. The other phases follow with a similar delay. The result is the oscillogram shown in Fig. 5c, with persistently negative peaks which do not cross into the positive region until the choke is completely discharged, as might be the case at point 5. The current trace in Fig. 5d shows that the reduction of current due to the discontinuities is less violent, but steady, so that the short circuit is safely eliminated in a shorter time.

It was mentioned that these processes are governed by the size of the smoothing choke. The saturation limit of the choke is a particularly important factor in this respect. In accordance with the law of induction, the short-circuit current rises more slowly if the inductance is high, and more quickly if it is low. In the oscillograms of Fig. 5b and 5d this is apparent

from the kink at the dashed line representing the saturation limit s . It is shown exaggerated in the diagram for reasons of clarity. If the choke has a greater saturation reserve, the short-circuit current would rise appreciably less. Apart from the cost of such a choke, however, one must also take account of any faults where the short circuit is not immediately interrupted. The maximum short-circuit current is determined by the internal resistance of the rectifier, and is usually about ten times the rated current. In such a case, a choke with a greater saturation margin would have stored a much greater quantity of energy, and clearing the short circuit would then be far more difficult.

If the saturation margin is small, the short circuit current rises beyond the saturation value even if the short circuit is eliminated quickly, but soon falls again during the recuperation period. With simple grid blocking, as in Fig. 5a, saturation is also indicated in the oscillogram (Fig. 5b) by the higher current peaks and the flat valleys.

Determining the Filter Size

The filter unit (Fig. 3) must meet certain requirements, and these are described briefly below.

Hum level

The usual stipulation that a transmitter should be free from hum at 60 dB means that the hum voltage at the rectifier output must be considerably less than 0.1 %. A certain minimum filter element is therefore necessary, in which case the determining factor is the product LC .

Natural frequency

This must be below the power frequency and below the lowest frequency transmitted, i.e. normally lower than 30 Hz. Again, the product LC is the deciding factor. If the natural frequency is set at approximately 20 Hz, the stipulation regarding hum will also be satisfied.

Starting current inrush

If the rectifier is turned on suddenly, a charging current surge flows to the filter capacitors and under certain circumstances can overload the rectifier tubes. This surge can be reduced by enlarging the induc-

tance and suitably decreasing the capacitance to acceptable values.

Internal impedance

The rectifier supplies the transmitter with a variable direct current which has alternating currents superimposed on it, of down to 30 Hz depending on modulation. If the modulation amplitude suddenly changes, current surges occur which must not have too great an influence on the d.c. output voltage. If a dynamic surge (change from one d.c. value to another) causes the filter to overshoot excessively, dynamic distortion occurs. Also, the a.c. load must not give rise to excessive a.c. variations of the d.c. voltage at the rectifier, so that the distortion remains within specified limits. A relatively large filter capacitor is needed to meet these requirements. The effects of the current inrush when the rectifier is switched on must then be reduced by increasing the voltage automatically and progressively, instead of by using a larger inductance.

Distortion factor

The distortion factor of a transmitter depends on its filter capacitance. This point requires careful examination. The basic circuit of a simple anode-modulated transmitter can be seen in Fig. 6. The rectifier supplies the RF stage 5 via the secondary of modulation transformer 3, and also, via the mid-point of the primary, the two AF tubes 4, both of which operate in class B. Modulation of the AF stage is superposed on the d.c. supply to RF stage 5 by means of the modulation transformer. There are then three distorting influences.

- Because of the two AF tubes operating in class B, two half-wave surges are drawn each cycle from the rectifier, as indicated by oscillogram 4.1 in Fig. 6, and passed to the final stage as a superimposed cycle (oscillogram 5.1). As a result of these half-wave surges from the rectifier there appears at smoothing capacitor 2 a second voltage harmonic which is added as a supply voltage to oscillogram 5.1. In other words, it causes second-harmonic distortion of the modulation in the RF stage.

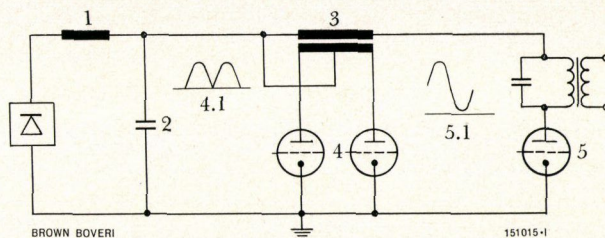


Fig. 6. – Simple anode-modulated transmitter

- 1 = Filter choke
- 2 = Filter capacitor
- 3 = Modulation transformer
- 4 = AF final stage
- 4.1 = Half-wave current surges per cycle from the rectifier to the AF stage
- 5 = RF final stage
- 5.1 = Voltage at RF stage

- Owing to the presence of this second harmonic at capacitor 2 (Fig. 6), one half-wave is processed in one of the AF tubes under anode-voltage conditions which are different from those in the second tube. This gives rise to distortion with the first and third harmonics. The first harmonic does not cause any non-linear distortion, but only affects the frequency response to some extent. Whereas this can easily be corrected, the third harmonic has a disturbing effect.
- The sinusoidal loading of the RF stage produces a natural-frequency voltage variation at the filter capacitor. This reinforces the difference in the way the two half-waves are handled in the AF stage, and the result is further distortion at the second harmonic.

All three kinds of distortion are directly dependent on the size of the filter capacitance 2 (Fig. 6). The first and third types of distortion described have the greatest influence on the transmitter, while the second type is of minor significance. The various forms of distortion can be calculated, and the required capacitance is ultimately determined by the maximum permissible distortion factor.

Rectifiers with Semiconductor Devices

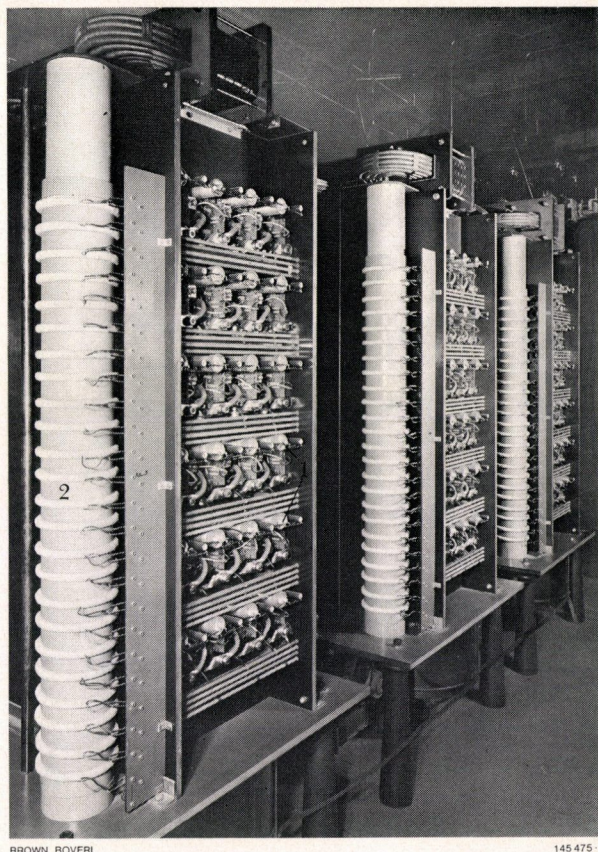
Semiconductor devices have been steadily improved in recent years, and have two advantages

over thyratrons. Firstly they last longer and, secondly, the mercury-vapour discharges in thyratrons are dependent on temperature, i.e. the anode voltage must not be turned on before a certain pre-heating time has elapsed, and the temperature has to be carefully monitored during operation. The unavoidable pre-heating time seriously complicates matters in the event of a power failure.

Rectifiers with Thyristors

Today thyristors can perform the same tasks as thyratrons. The following disadvantages, however, must be set against the merits of practically unlimited life and independence of temperature.

- The inverse voltages of thyristors are still appreciably lower than those of thyratrons. The value of the anode voltage therefore governs the number of thyristors which have to be connected in series.
- Thyristors (and diodes) are destroyed if subjected only once to excessive current or voltage. Thyratrons, on the other hand, are relatively insensitive in this respect and can tolerate a considerable number of backfires.
- With series-connected thyristors, care must be taken to ensure a uniform voltage distribution during the blocking period. All the thyristors must therefore be bypassed with high resistances. It is also possible to limit the voltage by means of avalanche diodes. Furthermore, it is necessary to balance out the voltage difference resulting from the delay in passing from the on-state to the off-state due to the hole-storage effect in the individual thyristors. This is achieved by series-connected damping resistors and capacitors for each thyristor.
- Thyristors are sensitive to rapid changes of current. Any change at the beginning of the conduction period or before blocking, i.e. when the current is small, must not be too quick owing to the risk of local overloading or conduction-through. This is because the speed at which the firing processes can spread is limited. With small currents, therefore, the rate of rise of the current must be reduced by inserting a choke which becomes immediately supersaturated if the current rises.



BROWN BOVERI

145 475-1

Fig. 7. - *Experimental thyristor rectifier for a 1000 kW transmitter*

- 1 = Thyristor units
- 2 = Firing transformer

- Each thyristor has to be controlled individually. Compared with a thyatron rectifier, therefore, the number of control points in each limb is greater and is equal to the number of series thyristors. To avoid voltage differences, it is important that all the thyristors in a limb fire at the same moment. Special firing transformers are needed for this. The problem will probably be simplified in the foreseeable future by using a flash of light to fire the thyristors.
- Mains overvoltage peaks must be kept away from the thyristors by fitting the rectifier transformer with capacitors or other means of absorbing alternating peaks.
- Rectifiers with thyristors are at present more expensive than those with thyratrons.

If the precautionary measures referred to are taken, thyristors can perform the same duties as thyatrons, and full advantage can be taken of the merits of gate control. Fig. 7 shows an experimental version of a thyristor rectifier for a 1000 kW transmitter. Each phase of the rectifier forms a separate unit, one limb being at the front, and the other at the rear. Each limb has six rows of four series-connected thyristors. These can clearly be seen in Fig. 7. The individual thyristors obtain their control pulses from the appropriate secondary winding of a special firing transformer 2 (Fig. 7). This consists of a single primary loop, which passes through the centre of an insulating tube, and of the rings discernible on the tube. Each ring constitutes an iron core and secondary winding for one thyristor.

Rectifiers with Semiconductor Diodes

Rectifiers with diodes are simpler and cheaper than those with thyristors. However, they cannot be used either to regulate the voltage or to disconnect short circuits. The switching functions must be carried out by circuit-breakers or other means of control. In the event of a short-circuit these cannot feed the energy of the choke back into the system. This energy always flows in full to the site of the short circuit because all the diodes conduct the short-circuit current in the forward direction. Moreover, because circuit-breakers cannot interrupt as quickly as controlled rectifiers, the short-circuit current usually reaches the steady-state value determined by the transformer leakage.

Protection with circuit-breakers

Stepwise turn-on is most easily accomplished with the aid of a star/delta connection on the primary side of the transformer. Diode rectifiers of this kind have been used for a long time in small transmitters. In the course of time they have been employed for ever higher transmitting powers. The question thus arises as to whether they are not also suitable for very high outputs. In the larger transmitters, however, the tubes are much more sensitive to short circuits, and any damage incurs a greater financial loss. Also, large circuit-breakers are generally slower than small ones. They need between three and five

cycles to extinguish an arc completely, whereas a grid control system can reduce the voltage to zero in approximately half a cycle. Only vacuum breakers are capable of interrupting relatively high currents inside one cycle. They cannot be used as primary breakers, however, because their capacity is limited, and is usually insufficient to interrupt short circuits on the primary side of a transformer, i.e. short-circuit currents determined by the network impedance.

Very high dangerous overvoltages can also occur, for example, when the transformer is open-circuited and the rectifier is at no-load. Nevertheless, vacuum breakers can be used to interrupt short circuits quickly if they are fitted on the secondary side of the transformer, together with the primary circuit-breakers. Tetrodes are being used increasingly for large transmitters. The screen grid of these reacts very quickly to short circuits. In such cases even a controlled rectifier often cannot guarantee the necessary protection, for with these, too, the capacitor energy flows to the short-circuit location.

Tube protection with crowbar systems

This situation can be improved with what are termed crowbar systems. These consist of controlled discharge gaps connected in parallel with the power capacitors. When a short circuit begins, the crowbar systems are switched to the conducting condition so

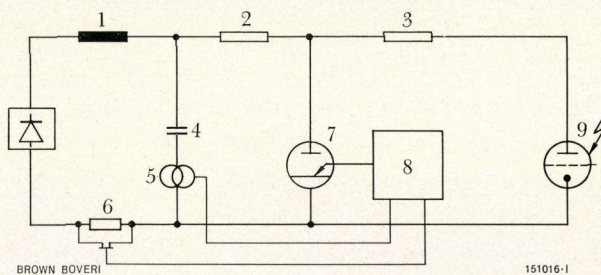


Fig. 8. — Rectifier circuit with crowbar protection

- 1 = Filter choke
- 2, 3 = Resistors
- 4 = Filter capacitor
- 5 = Transformer
- 6 = Shunt
- 7 = Ignitron
- 8 = Control unit
- 9 = Transmitting tube

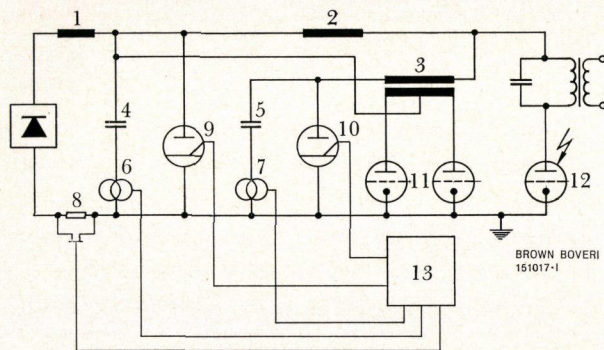


Fig. 9. - Transmitter circuit with crowbar protection

- 1 = Filter choke
- 2 = Modulation choke
- 3 = Modulation transformer
- 4 = Filter capacitor
- 5 = Modulation capacitor
- 6 = Transformer for filter capacitor 4
- 7 = Transformer for modulation capacitor 5
- 8 = Shunt
- 9, 10 = Ignitrons
- 11 = AF stage
- 12 = RF tube
- 13 = Control unit

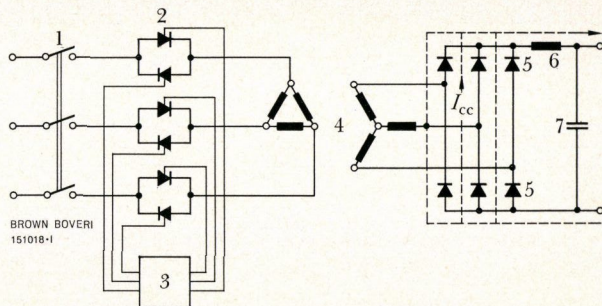


Fig. 10. - Rectifier with a.c. control circuit

- 1 = Primary breaker
- 2 = A.C. control circuit
- 3 = Control unit
- 4 = Rectifier transformer
- 5 = Rectifier diodes
- 6 = Filter choke
- 7 = Filter capacitor
- I_{cc} = Short-circuit current

that the capacitor energy can flow away before a significant proportion reaches the site of the short circuit. The simplest circuit is illustrated in Fig. 8. If tube 9 suffers a breakdown, the first current peak flows from capacitor 4 via resistors 2 and 3 and transformer 5. The latter sends a pulse to control unit 8 which triggers ignitron 7. The discharge current from capacitor 4 then flows via resistor 2 through ignitron 7, and tube 9 is protected not only against the remainder of the discharge surge from capacitor 4, but also from the subsequently increasing short-circuit current of inductance 1. This current can then be higher and longer without causing damage. In the event of short circuits which build up slowly, in which case the pulse produced by transformer 5 would be too small, the ignitron is relieved of the total current by means of shunt 6. The values of resistors 2 and 3 are comparatively low, so that their energy consumption is not significant, but at the same time they are high enough to ensure that the short-circuit current is accepted as fully as possible by the ignitron.

Ignitrons are very well suited to crowbar systems. The relatively high power required for control is not important because they are seldom in operation. On the other hand they require no power for heating when not in use, and their mercury-pool cathodes can tolerate high discharge currents.

The usual circuits for anode-modulated transmitters include a modulation capacitor 5 (Fig. 9), as well as a filter capacitance. If arc-over occurs in tube 12, the tube is subjected to the energy not only from capacitor 4 (via modulation choke 2) but also from capacitor 5 (via modulation transformer 3). With this arrangement, therefore, capacitor 5 must be discharged by way of another ignitron. It is also evident that, having started, the subsequent short-circuit current now flows across modulation choke 2 and on to the site of the short circuit. Ignitrons 9 and 10 (Fig. 9) are not able to intercept the short-circuit energy accumulated in modulation inductance 2. Under certain circumstances, therefore, another crowbar system has to be connected across this choke.

In contrast to medium-wave transmitters, short-wave transmitters require a controllable high voltage, because of the need to change wavelengths. Retuning is conveniently done at a low voltage, to reduce any risk of overloading. It is true that a star/delta connection is to a large extent adequate for this, but finer control is usually necessary. One reason why thyristor rectifiers are expensive is that with high voltages a large number of thyristors have to be connected in series, together with appropriate protective circuits. With a lower primary voltage, 380 V for example, control can be effected considerably more cheaply by means of a.c. control circuits. These now cost little more than electromechanical switches of the same capability. The circuit has the form shown in Fig. 10. On the primary side of the transformer are six groups of thyristors connected in antiparallel. With this

arrangement the voltage can be controlled with control unit 3 just as smoothly as with high-voltage control. However, in the event of a short circuit, an a.c. control circuit can interrupt the current only in the same manner as a circuit-breaker. In any diode rectifier the short-circuit current I_{sc} flows through the diodes, reinforced by the energy from the filter choke. An a.c. control circuit therefore also requires crowbar protection appropriate to the sensitivity of the tubes concerned.

Conclusion

For economical reasons, the majority of rectifiers for large transmitters are still fitted with thyratrons. Semiconductor devices, however, are steadily becoming better and less expensive, and the point will come in the near future when the main emphasis will swing to rectifiers employing thyristors or diodes.

(DJS)

M. DICK

Digital Path Simulator for Conveyor Systems

622.67-523.8:621.374

A digital path simulator for conveyor systems is described. It gives continuous indication of the position of the container and also enables control signals (e.g. for regulating the motion of the conveyor) to be obtained from various points along the track. These are created by a pulse generator, a counter and a decoder. Inaccuracies due to mechanical equipment are eliminated by a correcting device.

Purpose and Function of Path Simulation

Manual control of conveyor systems is currently used only in small, low capacity installations with low lift ratios, or if a fault occurs in an automatic system. If the requirements with regard to speed and stopping accuracy are stringent, or if the conveyor system is long and has a large number of stops, then usually for reasons of economy an automatic control system is employed which supervises the operating sequence of the installation by means of a path simulator. This provides a functional image of the actual conveyor configuration, i.e. all positions at which the sequence is required to change can be monitored by logic circuits and the necessary control commands derived.

In principle it is possible to provide mechanical path simulation by means of reduction gearing and cam switches. Controllers for mine winders are based on this principle. Mechanical play and unavoidable wear in the mechanical transmission components means that the reproduction of each control process deteriorates with time. Another factor is the limited resolution of the complete system by mechanical means. For these reasons there has been a general trend of late towards simulation by digital means.

When digital simulation is used the rope driving sheave is fitted with a pulse generator which emits a number of pulses proportional to the distance travelled by the container. If these pulses are counted in relation to the direction of rotation it is possible to instigate a control process by means of a coincidence pulse when a preset number is reached. This could, for instance, stop the container at any desired position.

The Necessity of Synchronizing and Correction

In order to overcome the fluctuations in the length of the rope due to varying loads, slip, changes in temperature, etc., the appropriate desired values for various positions along the journey are fed into a counter. The actual corresponding value is then set at the counter.

Where a sheave is used for winding the rope the transmission ratio between the pulse generator and driving sheave diameter varies due to wear between the sheave and the rope. The number of pulses emitted per unit length of travel therefore increases as the sheave diameter reduces. For this reason a test journey must be made periodically to determine the number of excess pulses. In order to prevent the accuracy of simulation from deteriorating, these excess pulses are eliminated by a correction. This correction is made by setting a number corresponding to the number of excess pulses counted during the test journey in a code switch which eliminates excess pulses evenly over the whole length of travel.

Principle

The basic principle is described using Fig. 1 to illustrate it. The pulses from pulse generator 1 pass through the noise suppressors 2 and arrive at the sense-of-rotation logic 3. This decides in which direction the main counter must count. From here the pulses pass through an AND gate, which is triggered by a correction logic 4, and enter the main counter 7. From here they pass into decoder 8. Subsequently, a logic 10 instigates evaluation by output relay 11 when the number of pulses counted coincides with the preset value.

Each synchronizing pulse from 5 corresponding to a given distance of travel is coded in 6 and sets the main counter to the corresponding value.

Main Sub-Assemblies

Travel/Pulse Conversion

The travel/pulse converter is driven by the driving sheave or rope drum through a friction wheel and the working distance to be measured is transmitted to the input shaft of the converter. Two discs, displaced by 90° el relative to each other and each having ten slots, are mounted on this shaft. These slotted discs control two oscillators by the fact that the oscillations remain undamped in the slots but are damped by the solid portions. The oscillations are rectified and each drives an amplifier with a push-pull output. There are thus two trains of pulses available at the output terminals of the pulse generator at 90° el to each other when the shaft rotates. The phases are either leading or trailing, depending on the sense of rotation.

Noise Suppressors and Signal Restorer

In order to prevent discrepancies in the actual number of counted pulses due to noise voltages, the transmission leads from the pulse generators to the electronic equipment are fitted with filter circuits whose capacitors render ineffective the noise voltage peaks which are usually of very brief duration. As this also reduces the flank gradient of the pulses these must subsequently be improved by signal restorers.

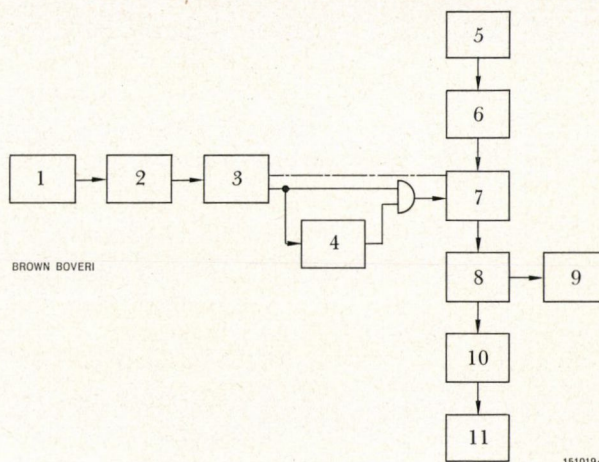


Fig. 1. - Basic circuit diagram for a digital path simulator

- 1 = Pulse generator
- 2 = Noise suppressors and signal restorer
- 3 = Sense-of-rotation logic
- 4 = Correcting logic
- 5 = Synchronizing pulse generator
- 6 = Encoding
- 7 = Main counter
- 8 = Decoding
- 9 = Digital display
- 10 = Logic
- 11 = Output relay

Sense-of-Rotation Logic

The two pulse trains which are displaced by 90° el relative to each other are fed into the sense-of-rotation logic which determines whether the drive is running forwards or backwards. On the basis of this decision the main counter receives a constant 0 or 1 signal which ensures that counting is carried out with the correct sign. At the same time as the sign decision is made the pulse train corresponding to the sense of rotation is selected and emitted for counting or correcting.

The two pulse trains from the travel/pulse converter have different lengths for the two senses of rotation. In order to standardize the pulses a timing element is incorporated which, when triggered, provides a pulse of constant length by changing from 0 to 1.

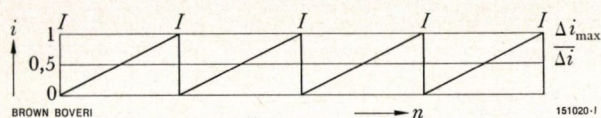


Fig. 2. - The effect of correction on the counting of excess pulses i

i = Excess pulses
 n = Journey
 I = Pulse elimination

Main Counter

The pulses emitted by the AND gate for counting arrive at a reversible binary counter which is triggered by the positive counting pulse flanks. Apart from the input for the counting pulses and the one for determining the sense of counting which is controlled by the sense-of-rotation logic, the counter also has a communal reset input and a setting input for each bit. The logic operates such that a synchronizing command resets the counter to zero and then sets it to the prescribed value. During this process the input for counting pulses is blocked to prevent faults which could arise from simultaneous setting and counting.

Correcting Logic

As has already been stated, excess pulses due to wear at the driving sheave must be prevented from arriving at the main counter input. The correcting logic which is fitted for the purpose of eliminating these excess pulses actually comprises two sections, one each for the X and Y correction. The simplest way to describe these corrections is by means of an example as follows.

Let us assume that

i_s = The number of pulses required for the total travel with maximum driving sheave diameter

i = Number of actual pulses counted during a test run over the whole journey

$i_m = i - i_s$ = Number of excess pulses

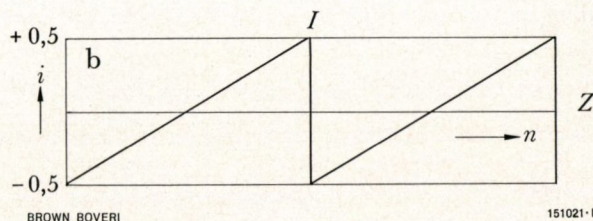
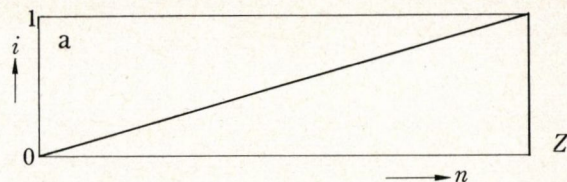


Fig. 3. - Improving correction by eliminating an additional pulse

a = Journey with one excess pulse
 b = Journey with two excess pulses
 i = Excess pulses
 n = Journey
 Z = End of journey
 I = Pulse elimination

We can now calculate after how many pulses a pulse must be eliminated in order to have eliminated exactly the right number at the end.

$$i_{X,Y} = \frac{i}{i_m}$$

With this method the error grows from zero until it corresponds to a full pulse and then one pulse is eliminated which means that the error is once again zero.

As illustrated by Fig. 2 the average error is half a pulse. In the worst possible case the error is a full pulse and the following trick is applied to overcome it. If one pulse more than is actually necessary according to the test-run is eliminated, the journey no longer commences with zero error, i.e. there is a built-in error before the journey starts. The average error over the whole journey is reduced to zero and the maximum error is only half of a pulse. This is illustrated by Fig. 3. For the sake of simplicity let us assume that one complete error pulse occurs over the total distance travelled (Fig. 3a). If the journey now commences with half a negative error pulse and if two pulses are eliminated over the journey (Fig. 3b) the maximum error is half a pulse.

affected by the output relays at certain counted sums or container positions. Definite preset values are compared with the registered number through AND or OR gates and when coincidence occurs a memory, provided for this purpose, is either set or reset, which through an amplifier causes the corresponding output to pick up or drop off.

Existing Plant

The digital control systems supplied with conveyor systems to Norway and Holland operate on the principle described above and comprise units of the Brown Boveri electronic system. They are returning excellent service.

(AH)

P. WOLF

The Resistivity of Insulating Oil in a Direct-Voltage Field

621.315.615.2.011.2

The resistivity of new and aged transformer oil in relation to field strength was investigated almost up to breakdown while varying the temperature, duration of the stress and flow velocity. The conductivity of aged oil follows simple laws, owing to the higher ion concentration, but certain anomalies are found with new oil, such as a maximum in the resistivity at 1 to 2 kV/mm, which can probably be attributed to space charge effects.

Insulating oil and oil-impregnated paper in various forms are the principal means of insulation in certain important items of equipment found in the rectifier and inverter stations of h.v.d.c. transmission systems. These items include the converter transformers and smoothing reactors, equipment for supplying auxiliary power and the control pulses, and to some extent also the thyristor valve groups and the transformer and wall bushings. Depending on its function and location, the insulation is subjected either to a straightforward d.c. voltage alone, or to a combination of d.c. voltage and a complex a.c. voltage. In many instances the insulation is of a composite structure consisting of one or more layers of solid insulating materials with oil-filled gaps in between.

With an electrical series arrangement of this kind, the partial voltage applied to each dielectric, in the case of d.c. voltage, is solely dependent on the d.c. conductances of the individual materials. These in turn are defined as the ratio of the leakage current to applied partial voltage. This current may also include proportions of a strongly time-dependent absorption current. The voltage distribution is very

much dependent on the properties of the insulating materials used, however, and also varies widely with time.

Origins of the Leakage Current

Absorption effects are to be expected first and foremost only in solid insulating materials as a result of almost inevitable inhomogeneities in their structure or composition. Such irregularities may, for example, be due to a laminated assembly or to the inclusion of particles having different dielectric properties in the main, homogeneous mass. With liquids, on the other hand, one would expect a similar situation only if particles are present in suspension. They should therefore be more amenable to investigation, thus making it easier to determine their electrical behaviour.

Current can flow in an absolutely pure insulating liquid only as a result of the release of electrons at the cathode due to photoelectric or field emission. In reality, however, the liquid always contains some kind of impurities, even though probably very finely distributed, and usually in dissolved form. Since these impurities tend to dissociate, positive and negative ions are continuously formed in equal numbers in the liquid until a balance, which is influenced by external circumstances, is achieved between the generation and dissipation of charge carriers, due to the processes of recombination and diffusion. The dissociation potential, and hence also the number

of ions bearing the current, is closely related to temperature. It increases rapidly with rising temperature.

Impurities in the liquid exert a decisive influence. These consist not only of suspended or emulsified foreign substances such as water, fibres and dust, etc., and sometimes also metallic salts which enter the oil through contact with the walls and electrodes of the container. They also include dissociation products due to ageing of the liquid. When a voltage is applied, these all contribute to electrical conduction in the basic medium, which is itself an ideal insulator. Mineral oils, which are mixtures of numerous paraffin and naphthene-based hydrocarbons together with a certain proportion of aromatically bound hydrocarbons, are particularly inclined to give rise eventually to organic acids, through bonding with atmospheric oxygen, and hence to constituents having an extremely high dissociation potential. This is especially so at elevated temperatures. Already in the initial stage of the ageing process, the so called induction period, when even sensitive chemical measurements are still unable to reveal any changes in the nature and composition of the liquid, electrical measurements—of conductivity, for instance, or dielectric loss factor—indicate the incipient modifications quite clearly. The results of electrical measurements depend to a large extent on the physical, mechanical and chemical purity, and hence on the degree of ageing, and also on temperature. Moreover, the behaviour of the oil may be further influenced by space charges near the cathode and anode which are created when current flows. In view of these numerous influencing factors and the fact that resistivity is extremely sensitive to only slight changes in the state of the measured liquid, one cannot expect the reproducibility of such measurements to be particularly high.

The relationship between the conductivity of mineral oils and these quantities in a weak d.c. voltage field has already been investigated. It has been found that the conductivity is greatly increased by water in droplet form dancing to and fro between the electrodes, and that with rising temperature a curve in the form of an inverted V is obtained for the function $\lambda = f(\vartheta)$ [1], owing to the increased solubility of water in the oil. It has also been estab-

lished that if voltage is applied for a considerable time (a matter of hours), conductivity decreases [2], and further that, when plotted against the ratio of field strength and electrode spacing, all measured values of ϱ obtained with an oil sample up to approximately 1 kV/mm lie on a curve which is influenced only by temperature, and which rises slowly at first and then more rapidly [3]. In greatly simplified terms, the main features of these observations, and also the occurrence of space charges, can be well explained by assuming singly charged positive and negative carriers of different mobilities in the liquid [3, 4].

Relationship between ϱ and $\tan \delta$

In an alternating field the loss factor $\tan \delta$, as measured in a high-sensitivity bridge arrangement, is used to characterize the degree of ageing of insulation oils, and to a lesser degree their purity as well. Usual temperatures and power frequencies are too low to cause significant losses due to orientation polarization, so that under these circumstances the conductivity determined with d.c. voltage only is decisive for the alternating field losses. Conversely, a value for the resistivity can be calculated from the loss indicated by the measured $\tan \delta$, and this resistivity agrees closely with direct measurement, at least in the case of oil which is not extremely pure [5].

By assuming spherical charge carriers of radius r and N in number, with charge $\pm Q$ and uniform velocity, the following expression for the loss factor can be derived from the equations of motion in a viscous medium of viscosity η (see Appendix):

$$\tan \delta = \frac{Q^2 N}{6 \pi^2 \eta r \varepsilon f}$$

where ε = Dielectric constant of the liquid
 f = Frequency of the applied voltage

Tests have also confirmed that the loss factor varies in inverse proportion to the frequency, while the losses themselves are independent of frequency.

To illustrate the definite relationship between the d.c. resistivity of an insulating oil and its dielectric loss factor, Fig. 1 shows the results of measurements at two temperatures with a considerable number of

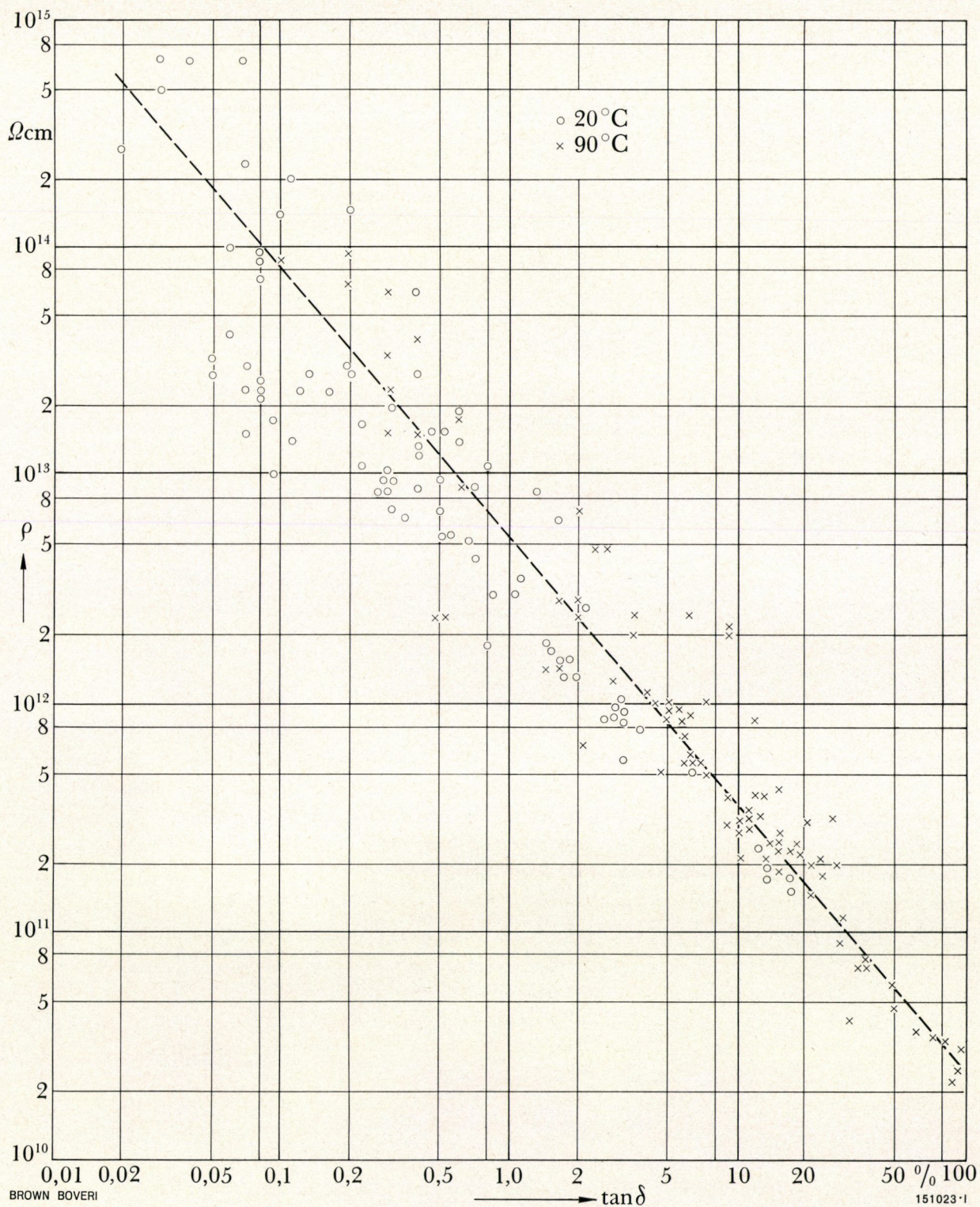


Fig. 1. – Relationship between specific resistance ρ and loss factor $\tan \delta$ for a total of 86 oil samples

Values measured at 20 and 90 °C [6].

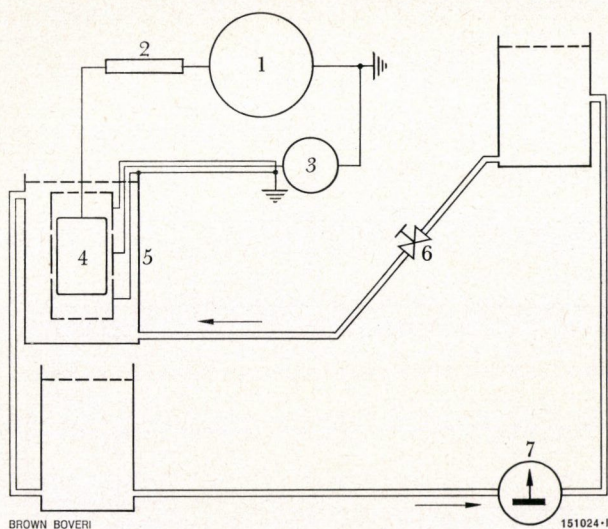


Fig. 2. — Test arrangement for measuring the resistivity of flowing insulating oil

- 1 = Voltage source
- 2 = Protective resistor
- 3 = Electrical picoammeter
- 4 = Measuring vessel
- 5 = Metallic screen
- 6 = Throttle valve for regulating flow velocity
- 7 = Reciprocating pump

oil samples from transformers of very different vintages and hours of operation, and thus covering a wide range as regards ageing. The values are plotted in double logarithmic coordinates, with $\tan \delta$ on the abscissa and the measured specific resistances ρ on the ordinate. The broken line representing the mean value conforms very well to the large number of individual measurements. From high values for ρ of about $10^{15} \Omega\text{cm}$ in the case of new oil ($\tan \delta_{90^\circ} = \approx 0.2\%$) the values drop by several orders of magnitude until, with severely aged oils, $\tan \delta$ ranges between 10 and 100% (measured at 90°C).

Measurements in Strong Fields

Little published information is available on the resistivity of insulating oils or similar liquids in a strong d.c. field almost up to breakdown. It has been found [7] that conductivity in an air-saturated liquid is greatly reduced, as is the emission of the cathode when irradiated. Also that the conductivity increases more than proportionally when the field strength is

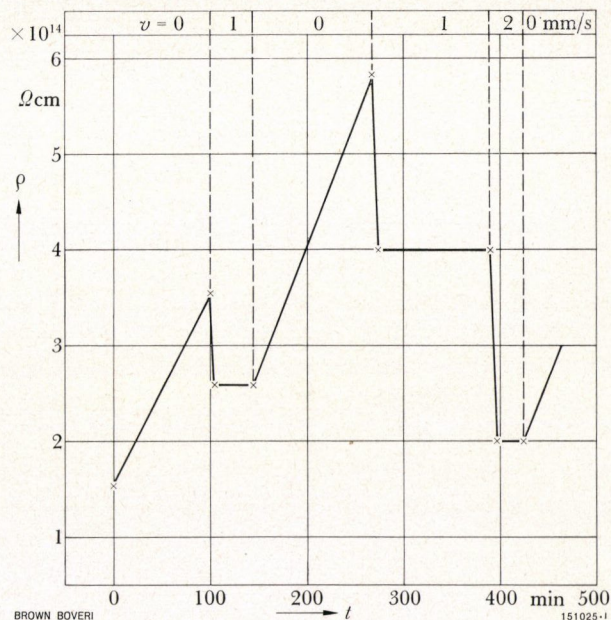


Fig. 3. — Resistivity of new oil in relation to time t and under the influence of flow velocity v

Measured at room temperature.

high [3], and that distortion of the field is also increased in front of the cathode [8]. In view of the considerable effect on the voltage stresses occurring in actual insulation arrangements with intermediate oil-filled spaces, it seemed appropriate to examine more closely the relationship between the resistivity and other properties of insulating oils of different origins and forms of pre-treatment. These measurements are discussed below.

Test Arrangement

For the tests we used two cylindrical measuring vessels, each with a fully screened measuring electrode. The effective oil volumes were 13.5 and 130 cm^3 , and the oil gaps 1 and 5 mm, respectively. Before each test the vessels were carefully cleaned and filled, but the oil sample was not put in under vacuum. For heat measurements the vessels were heated rapidly (in about 15 min) to 90°C in an oil bath.

Power was provided by a very stable, continuously variable electrostatic generator rated 80 kV and

0.2 mA, connected in series with a resistor of a few megohm. The leakage current was measured on the earth side with an extremely sensitive ammeter giving readings down to 10^{-14} A. All measuring lines were doubly screened, and great care was taken to exclude any other interference.

The specific resistance was calculated from

$$\varrho = \frac{U}{I} \cdot \frac{V}{(R-r)^2}$$

where V = Considered volume of oil

R, r = Outside and inside radii of oil gap

In some series of measurements the oil was circulated through the vessel by means of a pump in the external circuit (Fig. 2). It then flowed upwards through the vessel with a maximum velocity of 3 mm/s. The flow velocity could be regulated with a throttle valve.

The samples were proprietary oils of high technical purity (mean breakdown strength, measured in accordance with IEC, not less than 60 kV/2.5 mm, $\tan \delta_{90^\circ}$ not greater than 0.4%), with an aromatics content of less than 13%, and also aged oils taken from transformers with $\tan \delta$ values of 8 and 37%. These latter oils were also in good condition as regards purity, and had high electric strengths. The air content of all the oils was between 30 and 80% of saturation.

Results

Influence of Test Duration and Flow

When the voltage applied to still, new oil is constant, the resistivity measured increases at first. A value roughly 8 times higher is reached after one to two days. This relationship to time seems to be more pronounced with a weak field (below 0.5 kV/mm).

In the case of aged oils, on the other hand, the final state is reached immediately, as is so with moving new oil. This feature of new oil is illustrated in Fig. 3. Once the voltage is applied, the resistivity of the still oil rises in about 100 min to approximately double its initial value. If only a slight movement is imparted to the oil, the resistivity immediately drops

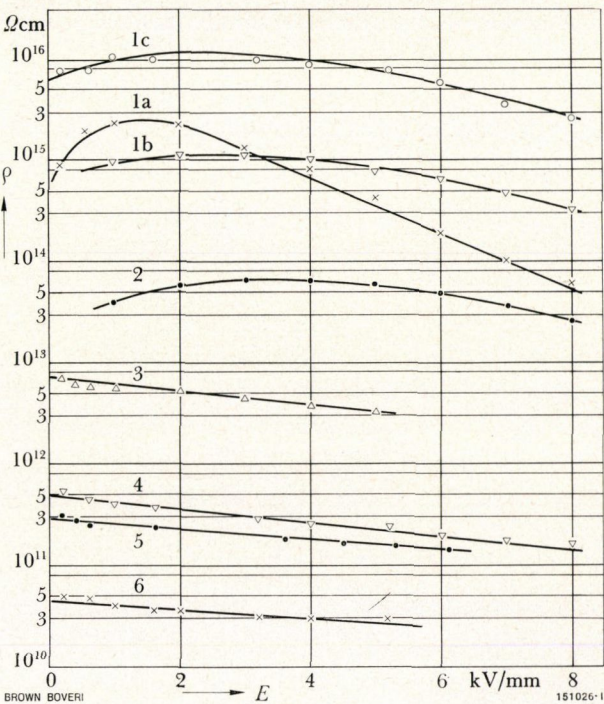


Fig. 4. - Specific resistance of transformer oils in relation to field strength

Except for curve 1a, all curves were obtained with the 5 mm measuring vessel.

- 1a = Voltage applied for 20 min previously. Mean of several measurements
 $\vartheta = 20^\circ\text{C}$
- 1b = As 1a, but vessel with 1 mm oil gap
- 1c = As 1a, but voltage applied for several days beforehand
 $\vartheta = 20^\circ\text{C}$
- 2 = As 1a, but $\vartheta = 90^\circ\text{C}$, mean of several measurements
- 3 = $\tan \delta_{90^\circ} = 8\%$, 20°C
- 4 = $\tan \delta_{90^\circ} = 37\%$, 20°C
- 5 = $\tan \delta_{90^\circ} = 8\%$, 90°C
- 6 = $\tan \delta_{90^\circ} = 37\%$, 90°C

to a much lower, and practically constant value. The drop is greater when the flow velocity is higher. As soon as the oil stops moving, the resistivity increases again.

The Influence of Field Strength

With a technically pure insulating oil in a d.c. voltage field, breakdown can be expected to occur at a field strength of about 12 kV/mm, or slightly

higher [9]. It was therefore of interest to examine the resistivity of new and aged oil at room temperature and in the region of transformer operating temperatures with field strengths up to approximately 8 kV/mm.

A selection of the curves thus obtained are shown in Fig. 4. The resistivity of still, new oil at room temperature increases at first with field strength until, beyond about 2 kV/mm, it drops again more or less rapidly, depending on the duration and magnitude of the preceding exposure (curves 1a and 1c). The decrease is smaller in the vessel with a 1 mm oil gap (curve 1b) than in the larger with a 5 mm gap (curve 1a). When the sample was subjected for several days to a field strength corresponding to just less than the breakdown limit, the resistivity increased as expected (curve 1c). The maximum of the curve of $\rho = f(E)$ is less pronounced.

The resistivity of new oil heated to 90° and subjected to no previous stress varies very little with field strength over the whole range (curve 2). In consequence, the difference in resistivity between hot and cold oil in a strong electric field is only a factor of about 2, instead of between 10 and 15, as would otherwise be the case.

With old oil the resistivity decreases monotonically with increasing field strength throughout the considered range. The values attained are then lower, the greater the ion concentration, i.e. as the ageing process is more advanced (measured in terms of $\tan \delta$), or the oil temperature is higher.

In general, the following expression is valid in the region of diminishing resistivity:

$$\rho = \rho_0 \cdot e^{-\beta E}$$

in which ρ_0 is a reference value when extrapolating to a very low field strength. From the measurements illustrated in Fig. 4 we obtain the following numerical values for β :

$$\text{Curve 1a} \quad \beta \approx 0.64 \text{ mm/kV}$$

(In a total of 8 series of measurements on various new oils, β was between 0.5 and 0.85 with field strengths between 2 and 8 kV/mm.)

$$\text{Curves 3 and 4} \quad \beta \approx 0.14$$

$$\text{Curves 5 and 6} \quad \beta \approx 0.10$$

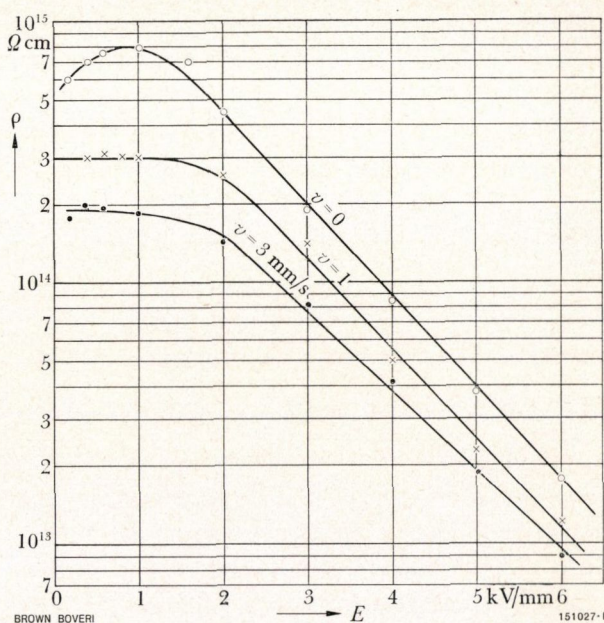


Fig. 5. – Resistivity of flowing transformer oil in relation to field strength at different flow velocities

Oil gap 5 mm
Temperature 20 °C

When the 5 mm vessel was refilled with a new oil from another source, the curve denoted $v = 0$ in Fig. 5 was obtained under the same conditions of measurement as for curve 1a in Fig. 4.

With somewhat lower absolute values of the resistivity the drop is rather greater at high field strengths. When the oil in the gap is made to flow, the resistivity drops in accordance with the pattern shown in Fig. 3, and the maximum at about 1 kV/mm disappears. Below this value the resistivity is constant.

Influence of Temperature

The known effect of temperature, described by the expression

$$\rho_{\vartheta} = \rho_0 \cdot e^{-\alpha \vartheta}$$

was also examined in relation to aged oils. The results of measurement with three varieties of oil are shown in Fig. 6. The three samples were new oil, slightly aged oil ($\tan \delta_{90^\circ} = 8\%$) and more severely aged oil ($\tan \delta_{90^\circ} = 37\frac{1}{2}\%$). All were measured at 20 and 90 °C with field strengths of 1 and 5 kV/mm.

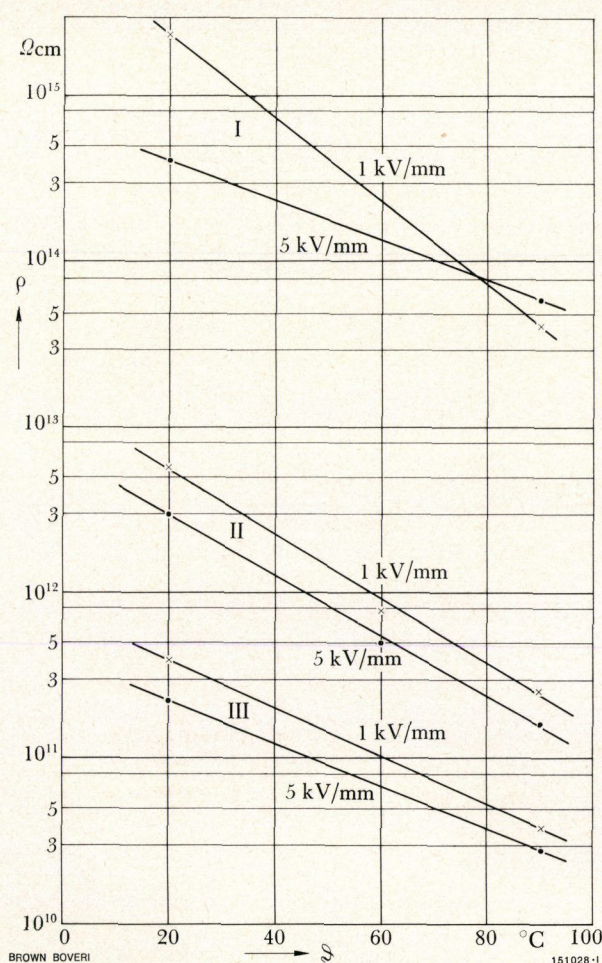


Fig. 6. — Resistivity of transformer oil in relation to temperature θ , with degree of ageing ($\tan \delta$) and field strength as parameters

Measurements taken after brief application of voltage (a few minutes). Oil gap 5 mm.

I = New oil at 1 kV/mm, $\alpha = 0.057 \text{ deg C}^{-1}$
at 5 kV/mm, $\alpha = 0.027 \text{ deg C}^{-1}$

II = $\tan \delta = 8\%$, $\alpha = 0.045 \text{ deg C}^{-1}$

III = $\tan \delta = 37\%$, $\alpha = 0.030 \text{ deg C}^{-1}$

In the case of the aged oils, exponent α is independent of field strength, and is influenced only by the type of oil and its previous history. With a new oil, however, the effect of temperature on resistivity is less marked in a strong field than in a weak one. This is not so with oil subjected to a field for a period of days beforehand. Here, α is higher and unaffected by the field. Values for α obtained from Fig. 6 vary between 0.057 and 0.027 per deg C,

which means that at 90 °C the resistivity is equivalent to $1/50$ or $1/7$ of the values at 20 °C.

Discussion of Results

New insulating oils of high technical purity, characterized by specific leakage resistances above $10^{13} \text{ } \Omega\text{cm}$, are very easily affected as regards their dielectric behaviour by a wide variety of external influences. Apart from impurities originating from outside or from the walls of the container, the main influencing factors are temperature, the duration and magnitude of the applied d.c. field, and movement of the oil. New oil may also be affected to some extent by photoionization and photoelectric emission at the cathode, and hence by the cathode material and the cleanliness of the surface.

The action of all these factors can be explained by assuming that the oil contains dissolved impurities capable of dissociation. Because of their dissociation potential, positive and negative ions or colloidal ion complexes having one or more times the electronic charge are formed and slowly migrate in the electrical field towards the electrodes. This charge displacement represents a current. As the temperature rises, the number of ions increases rapidly, together with the electrical conductivity of the liquid. Above all, charges of opposite sign accumulate near the respective electrodes. The consequent polarization of the liquid causes the potential to vary more rapidly in the vicinity of the electrodes, and flatten out in the broad central portion which supplies the ions. The result is that the transport of carriers is impeded, and the resistivity gradually increases (Fig. 4). The same effect is created by the migration of carriers from the volume of the liquid to the electrodes, and their discharge and deposition there.

Because of the very slight mobility of the carriers, and hence the low rate of adjustment of these effects, even moderate movement of the oil has the result of removing space charge layers already formed and of bringing new carriers into the oil exposed to the electrical field, and the original state of increased conductivity is therefore quickly restored (Fig. 3).

Because the ion concentration in aged oils, on the other hand, is far greater, the conductivity is much

higher, and the electrical behaviour is much less easily influenced. In view of the large excess of dissociable molecules, no significant effects dependent on time or movement are to be expected.

The deviation from Ohm's law, studied here for the first time in detail, in that the resistivity of new oil in a weak and a strong electrical field varies in opposite directions, and that a pronounced maximum occurs between 1 and 2 kV/mm, especially at low temperatures, may have a number of different causes. The initial increase with field strengths up to about 1 kV/mm can be explained by assuming there are two kinds of charge carrier and that only dissociation occurs, i.e. disregarding recombination effects [3]. The drop in resistivity at high field strengths may be due to weakening of the space-charge field distortion or to an increase in ion mobility with field strength. It may also be the result of field-induced dissociation in the body of the liquid or field-induced photoelectric emission at the cathode. Which of these influences predominates, or whether other effects also play a part, cannot be established from the measurements carried out. Also, further measurements must be made in order to determine whether the statements made here concerning resistivity in conjunction with bare electrodes can be applied direct to the behaviour of insulating oil in enclosed spaces.

The tests described were carried out under the auspices of the HVDCT Working Group, comprising AEG, Brown Boveri and Siemens.

(DJS)

B. GÄNGER
G. MAIER

Appendix

Relationship between Loss Factor and Conductivity

Let us assume that the insulating liquid contains only spherical charge carriers of mass m and diameter $2r$, each having a charge Q . In an alternating electrical field $E_0 \sin \omega t$ of frequency $f = \omega/2\pi$, each particle is acted upon by a force

$$F_1 = QE_0 \sin \omega t$$

where

$$E_0 = U_0/d$$

Movement in the viscous medium is retarded by friction force F_2 . According to Stokes' law:

$$F_2 = 6\pi\eta rv$$

where $v = ds/dt$ denotes the velocity of the particle in the direction of the field, and η is the viscosity coefficient.

The particle thus obeys the equation of motion

$$m \frac{dv}{dt} = QE_0 \sin \omega t - 6\pi\eta rv$$

or

$$\frac{d^2s}{dt^2} + a \frac{ds}{dt} + b \sin \omega t = 0$$

where

$$a = \frac{6\pi\eta r}{m} \quad b = -\frac{QE_0}{m}$$

which has the solution

$$s = ce^{-at} + \frac{ab}{\omega(a^2 + \omega^2)} \cos \omega t + \frac{b}{a^2 + \omega^2} \sin \omega t$$

for the distance travelled by the particle in a given time. The first term on the right-hand side characterizes the rate of adjustment to changed test conditions, and is considered no further here. Also, it can easily be shown that for normal service frequencies $a \gg \omega$, and so for the transient state it is true as an approximation that

$$s = \frac{QE_0}{6\pi\eta r} \left(\frac{1}{\omega} \cos \omega t + \frac{m}{6\pi\eta r} \sin \omega t \right)$$

In one half-wave the particle travels a distance of

$$s_{(t=\pi/\omega)} = \frac{QE_0}{6\pi\eta r\omega} = \frac{QU_0}{6\pi\eta r\omega d}$$

Work

$$A = \int_0^s F_1 ds$$

is imparted to it by the external field. When

$$ds \approx \frac{QE_0}{6\pi\eta r} \sin \omega t dt$$

we have

$$A = \frac{(QE_0)^2}{6\pi\eta r\omega} \cdot \frac{\pi}{2}$$

If unit volume (1 cm^3) contains $2N$ positive and negative particles, these acquire work

$$A' = \frac{(QE_0)^2 N}{6\eta\omega r}$$

which corresponds to a power loss

$$P'_\omega = \frac{A'}{\pi/\omega} = \frac{(QE_0)^2 N}{6 \pi \eta r}$$

Referring this to the reactive power of unit volume in the electrical field

$$P'_b = \frac{1}{2} \omega \epsilon E_0^2$$

we obtain the desired relationship for the loss factor

$$\tan \delta = \frac{Q^2 N}{6 \pi^2 \epsilon \eta r f}.$$

Bibliography

- [1] A. W. STANNETT: The conductivity of hydrocarbon transformer oil containing water and solid conducting particles. Brit. J.appl.Phys. 1951, Vol. 2, p. 110-14.
- [2] J. L. ONCLEY, W. C. HOLLIBAUGH: Low voltage d.c. measurements on electrical insulating oils. Elect.Engng 1940, Vol. 59, p. 625-41.
- [3] N. L. HARRISON: Resistivity of transformer oil at low and medium field strengths. Proc. Instn elect. Engrs 1968, Vol. 115, p. 736-41.
- [4] J. GAVIS: Electrical conductivity of low dielectric constant liquids by d.c. measurement. J.chem.Phys. 1964, Vol. 41, p. 3787-93.
- [5] J. COQUILLION: Contrôle des isolants liquides par des mesures de résistivité et de pertes diélectriques. Rev.gén.Elect. 1964, Vol. 79, p. 603-14.
- [6] B. GÄNGER: Kontrolle der Isolierölalterung und Pflege des Öles von Hochspannungstransformatoren und Messwandlern. Elektrotech.Z. Series A 1963, Vol. 84, p. 800-03.
- [7] T. R. HESKETH, T. J. LEWIS: Electrical conduction in hexane and decane liquids using a crossed wire electrode system. Brit.J.appl.Phys. (J.Phys.D) Series 2, 1969, Vol. 2, p. 557-66.
- [8] D. W. GOODWIN: Space charge phenomenon in liquid dielectrics. Proc.phys.Soc. Section B 69 pt I 1956, p. 61-9.
- [9] B. GÄNGER: The breakdown voltage of oil gaps with high d.c. voltage. IEEE Trans. Pwr Appar. & Syst. 1968, Vol. 87, p. 1840-43.

The Accuracy of Calorimetry in Air Flow Measurement

681.121.8.082.53

It is general practice to use standard nozzles for determining the mass of air flowing through electrical machines. The characteristic values of these nozzles are the subject of many publications and are contained in international standards. While conforming to the relevant specifications accuracy deviations of only ± 1 to 2% can be attained which are usually adequate for technical purposes. The drawbacks of this method are the large pressure drop across the nozzle and the long ducts necessary to provide a good velocity profile. Both of these drawbacks can be overcome by using the calorimetry method of measurement. As will be demonstrated in the following, results obtained with standard nozzles agree well with those arrived at by calorimetry.

Scope

The total losses of a range of air cooled electrical machines have already been measured by calorimetry [4]. Here the mass of cooling air was determined by calorimetry, i.e. by measuring the temperature rise of the cooling air, because it was impossible to carry out measurements with nozzles due to the high pressure losses.

To supplement these tests another series of investigations was carried out and these show the agreement between the standard nozzle and air calorimetry methods. The measured range covers 0.5 to 3.5 kg/s which corresponds to the mass of cooling air for medium-size machines.

A further series of tests shows the agreement between the values obtained by calorimetry and those with the corresponding standard nozzles even where

the air and temperature distribution over the cross section of the measuring duct are not even. This enables the maximum error with air calorimetry due to these variations to be determined.

Principle and Assumptions

The mass of air flowing across the duct cross section is to be determined by air calorimetry. To this end the air was heated and the temperature was measured by a very accurately controlled resistance element before and after heating. In the steady-state condition therefore, the mass of air flowing is

$$q_m = \frac{1}{c_{pm}} \cdot \frac{P_H}{\Delta\vartheta} \quad (1)$$

where

$$q_m = \text{Mass of air flowing} \quad \left[\frac{\text{kg}}{\text{s}} \right]$$

$$P_H = \text{Heat output} \quad [\text{kW}]$$

$$\Delta\vartheta = \text{Mean temperature rise of the air due to } P_H \quad [\text{deg C}]$$

$$\Delta\vartheta = \vartheta_2 - \vartheta_1$$

and

$$\vartheta_1 = \text{Mean air temperature before heating} \quad [^\circ\text{C}]$$

$$\vartheta_2 = \text{Mean air temperature after heating} \quad [^\circ\text{C}]$$

$$c_{pm} = \text{Mean specific heat of the air in the range } \vartheta_1 \text{ to } \vartheta_2 \quad \left[\frac{\text{kJ}}{\text{kg deg C}} \right]$$

$$c_{pm} = (c_{p2} - c_{p1}) \cdot \frac{\vartheta_1}{\Delta\vartheta} + c_{p2}$$

It is assumed that the potential and kinetic energy of the air do not vary along the measured distance and that there are no heat losses or leaks. Also the air temperature must be constant across the duct cross section. Only then is equation (1) accurate; this was shown in [4].

Although it is a simple matter to determine the heat output, this is not the case with the uniformity with respect to time. On the other hand it is difficult to measure the air temperature before and after the heating element. This was achieved with resistance measuring grids which have thin nickel wires suspended across the duct cross-section [4].

The temperature sensitivity of the nickel wires is represented by an approximation polynomial

$$R = a + b\vartheta + c\vartheta^2$$

and the unknown coefficients a , b and c were determined by measurements carried out in an oil bath and varying the temperature [4].

If two measuring grids G_1 and G_3 are connected to a special Wheatstone bridge the temperature rise due to heating the air can be determined according to [4]:

$$\Delta\vartheta = \frac{1}{2} \cdot (\sqrt{A^2 + 4B} - A) \tag{2}$$

where

$$A = 2\vartheta_1 + \frac{b}{c}$$

$$B = \frac{\Delta R_3}{80.0 + R_{3_0}} \cdot \left(\frac{a}{c} + \frac{b}{c} \vartheta_1 + \vartheta_1^2 \right)$$

- ϑ_1 = Temperature before heating
(air inlet temperature)
- R_{3_0} = Reference resistance of two measuring grids
(e.g. $R_{G_{3-1}}$) i.e. the resistance recorded at the Wheatstone bridge without heating the air
- ΔR_3 = Increase in resistance at the same measuring grid due to heating air through P_H

According to equations (1) and (2) therefore, the heat output P_H , the specific heat c_{pm} and values ϑ_1 , R_{3_0} and ΔR_3 must be determined for calorimetric measurement of air mass q_m . Considerable difficulties are often involved in keeping the air inlet temperature constant while the air heating process is in the steady-state condition.

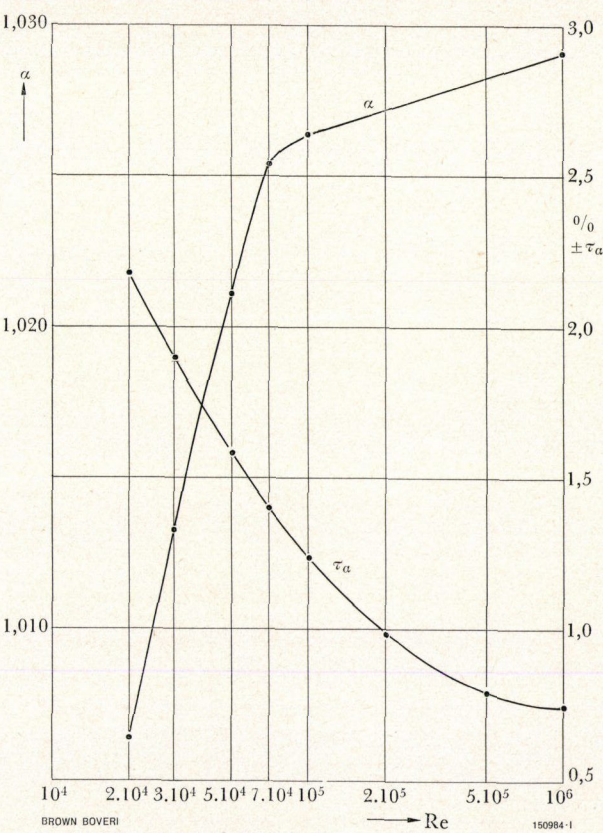


Fig. 1. – Flow coefficient α and tolerance τ_α in relation to Reynolds number Re

$$\text{Aperture ratio of standard nozzle } m = \frac{d}{D} = 0.3515$$

In order to check the accuracy of the calorimetric method the air flow masses were also measured using standard nozzles. A standard nozzle with an aperture ratio of $m = 0.3515$ was available for the flow rates in question, i.e. 0.5 to 3.5 kg/s, and the duct diameter D was 0.45 m. The flow coefficient α and expansion coefficient ε of the nozzle are given in DIN standards [1]. The interpolated values of α and ε for the nozzle used are given in Fig. 1 and 2. It was unfortunately not possible to calibrate the nozzle accurately using water because of the expense involved. The effect of surface roughness of the test ducts on the flow coefficients was so small as to be negligible.

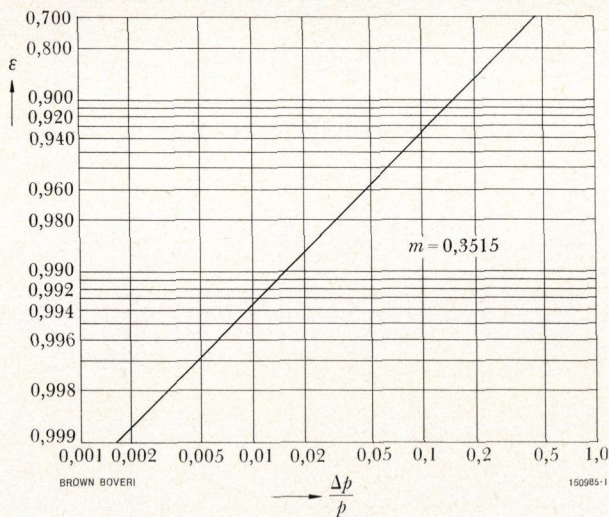


Fig. 2. — Coefficient of expansion ϵ in relation to the ratio of difference in static pressure at nozzle to pressure before the nozzle $\frac{\Delta p}{p}$

Aperture ratio $m = 0.3515$.

According to [1] the mass flow of air can be calculated as follows:

$$q_m = \alpha \cdot \epsilon \cdot \pi \cdot \frac{d^2}{4} \cdot \sqrt{2 \cdot \rho \cdot \Delta p} \quad (3)$$

where

d = diameter of nozzle aperture [m]

Δp = difference in static pressure at nozzle $\left[\frac{\text{N}}{\text{m}^2} \right]$

$$\frac{1 \text{ N}}{\text{m}^2} \approx 0.102 \text{ mm w.g.}$$

ρ = density of moist air $\left[\frac{\text{kg}}{\text{m}^3} \right]$

Tests and Results

The arrangement of the test apparatus is shown in Fig. 3. The air is sucked in through a plastics duct by fan 6. It then passes through a duct having a length approximately equal to twelve diameters

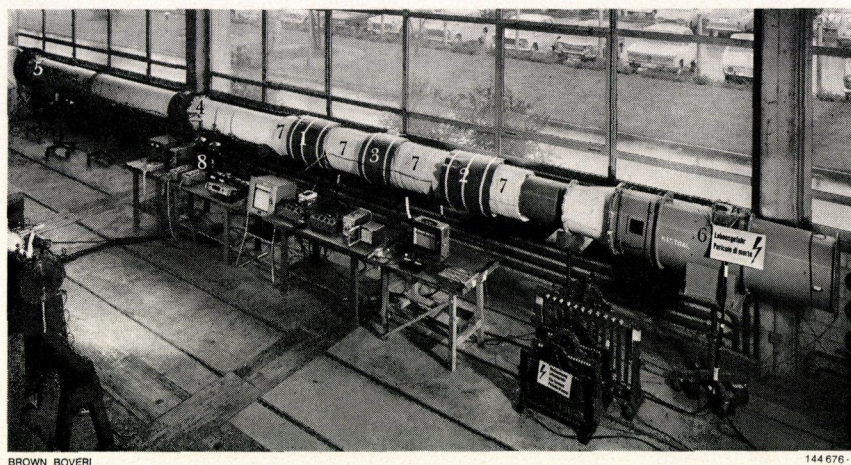
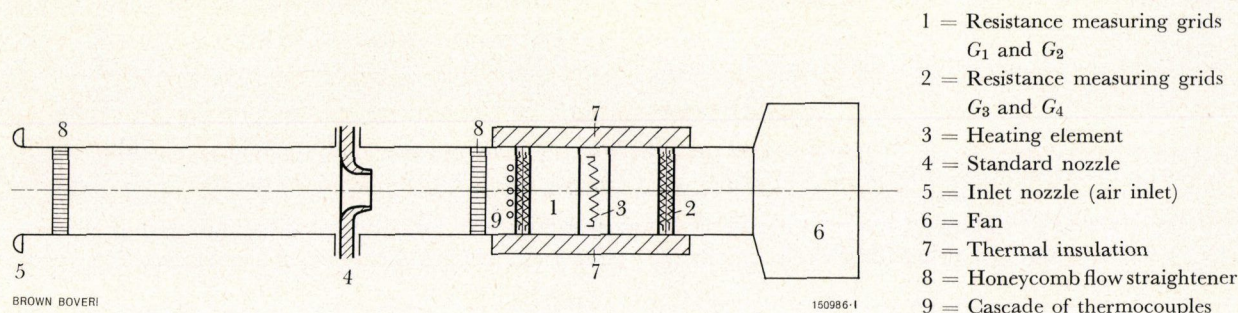


Fig. 3. — Arrangement of apparatus

- 1, 2 = Resistance measuring grids
- 3 = Heating element
- 4 = Standard nozzle
- 5 = Inlet nozzle (air inlet)
- 6 = Fan
- 7 = Thermal insulation
- 8 = Micromanometer

Fig. 4. — Diagrammatic arrangement of apparatus



($12 \times D$) and flows through a built-in standard nozzle. From here it passes through another duct of approximately eight diameters length and arrives at the heating element which forms the first obstacle.

The actual measuring grids are arranged symmetrically on either side of the heating element (Fig. 4) at a distance of two diameters. Immediately in front of grids G_1 and G_2 is a cascade of thermocouples which determine the air inlet temperature. The stretch of ducting from the cascade to measuring grids G_3 and G_4 , i.e. the actual calorimetric measuring distance, is clad with thermal insulation. As can be seen in the illustration, honeycomb flow straighteners are fitted in the duct to improve the air distribution.

Whereas a total length of ducting of $12 D + 6 D$, which is considered a minimum in the standards, was necessary for the tests involving nozzles, the calorimetric measuring duct was only $4 D$ long.

The difference in static pressure at the nozzle was measured with a precision micromanometer. This instrument has a range of 0 to 300 mm w.g. and readings can be taken with an accuracy of 0.01 mm of water. It was, however, never possible to attain such a high reading accuracy because of unavoidable fluctuations in the speed of the fan.

Table I shows the air flow values as measured by calorimetry and with a standard nozzle. The barometric pressure and relative humidity were virtually constant throughout the tests and the air inlet temperature varied between 23 and 27°C. The mean specific heat of the air c_{pm} was approximately 1.01 kJ/kg °C and the average density ρ was about 1.13 kg/m³.

As the heating element was inadequately designed the temperature rise $\Delta\theta$ dropped from about 12 to 5 deg C as the mass flow or air velocity increased.

TABLE I
Air flow measured by standard nozzle and calorimetric methods

Test No.	Reynolds No.	Air humidity	Density of moist air	Difference in static pressure at standard nozzle	Mass of air measured by standard nozzle	Increase in air temperature	Mass of air measured by calorimetry	Mean difference between air masses
	Re. 10^5	φ	ρ	Δp_N	$(q_m)_N$	$\Delta \theta_K$	$(q_m)_K$	$\frac{d(q_m)}{(q_m)_N}$
		%	kg/m ³	mm/H ₂ O	kg/s	deg C	kg/s	%
1	0.86	42	1.135	3.5	0.506	10.60	0.505	0.2
2	1.7	36	1.128	13.0	0.974	12.89	0.959	1.5
3	2.6	34	1.122	30.0	1.474	8.55	1.446	1.9
4	2.8	36	1.124	40.0	1.702	8.64	1.675	1.6
5	3.4	32	1.132	54.0	1.981	5.88	1.956	1.3
6	4.3	35	1.122	83.0	2.442	6.53	2.395	1.9
7	5.0	36	1.107	119.0	2.901	5.47	2.861	1.4
8	5.9	23	1.126	163.0	3.414	5.32	3.369	1.3

TABLE II
Determining the temperature rise of the air with four measuring grids

Test No.	Difference in air temperature between				Mean difference between air temperature increases $\frac{d(\Delta\theta)_{\max}}{\Delta\theta_{3-1}}$
	grids 3-1 $\Delta\theta_{3-1}$	grids 3-2 $\Delta\theta_{3-2}$	grids 4-1 $\Delta\theta_{4-1}$	grids 4-2 $\Delta\theta_{4-2}$	
	deg C	deg C	deg C	deg C	
1	10.60	10.59	10.55	10.55	0.5
2	12.89	12.84	12.86	12.83	0.5
3	8.55	8.50	8.50	8.51	0.6
4	8.64	8.66	8.64	8.62	0.5
5	5.88	5.89	5.85	5.84	0.9
6	6.53	6.50	6.48	6.50	0.8
7	5.47	5.46	5.46	5.49	0.6
8	5.32	*	*	*	—

* not measured

It can be seen from Table I that the mean error between the two sets of tests $d(q_m)/(q_m)_N = 1.5\%$. No definite reason for the obvious systematic deviation could be found without an elaborate calibration of the standard nozzle used. It is possible that the air flow determined by the nozzle was excessive and according to [1] this would cause the α values to be too great. Comparative measurements with various standard nozzles tend to confirm these suspicions.

In order to establish experimentally the error in the calorimetric determination of the temperature rise, pairs of measuring grids were fitted before and after the heating element. The result is four temperature readings ($\Delta\theta_{3-1}$, $\Delta\theta_{3-2}$, $\Delta\theta_{4-1}$ and $\Delta\theta_{4-2}$) per test. These are reproduced in Table II. As shown in Fig. 6 the maximum error between these values is 0.9%. (In Table I reading $\Delta\theta_{3-1}$ is used in every case for determining the air flow by calorimetry.)

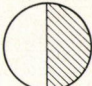
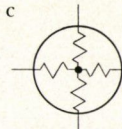




The connections between the measuring grids, two Wheatstone bridges and two null galvanometers are shown in Fig. 5. Connecting the null detector 4 to the recorder 5 enabled the temperature

fluctuations to be integrated for two measuring grids for the steady-state condition.

Another set of tests was carried out to determine the effects of any unevenness in air speed or temperature distribution on the accuracy of the air calorimetry method. In order to create an unsymmetrical flow at the measuring area half the duct cross section was closed immediately in front of measuring grids 3 and 4 during tests 9 and 10 (Table III) by a cardboard sheet. Although both the fluctuations in the effective pressure at the manometer and the variations in ΔR_3 were considerably higher in the steady-state condition, the error $d(q_m)/(q_m)_N$ between the two methods remained of the same order as before. It was not until the temperature distribution over the cross section was made unsymmetrical by heating only half of the element, as in tests 11 to 13, that considerable errors were recorded. Where the energy distribution over the duct cross section is so uneven, equation (1) no longer applies. With air calorimetry such unsymmetries are to be avoided and this can generally be arranged. Air calorimetry is therefore

TABLE III

Calorimetric air measurements with unsymmetrical air or temperature distribution over the duct cross section

Test No.	Difference in static pressure at standard nozzle Δp_N	Mass of air measured at standard nozzle $(q_m)_N$	Increase in air temperature $\Delta \theta_K$	Mass of air measured by calorimetry $(q_m)_K$	Mean difference between air masses $\frac{d(q_m)}{(q_m)_N}$	Duct cross section	Heating element
	mm/H ₂ O	kg/s	deg C	kg/s	%		
9	54.0	1.986	3.29	1.973	0.7	a 	c 
10	54.0	1.989	5.79	1.975	0.7		
11	54.0	1.990	3.72	1.844	7.3	b 	d 
12	54.0	1.990	8.33	1.864	6.3		
13	54.0	1.996	1.21	1.493	25.2	a  BROWN BOVERI	d  151164-1

a = half closed

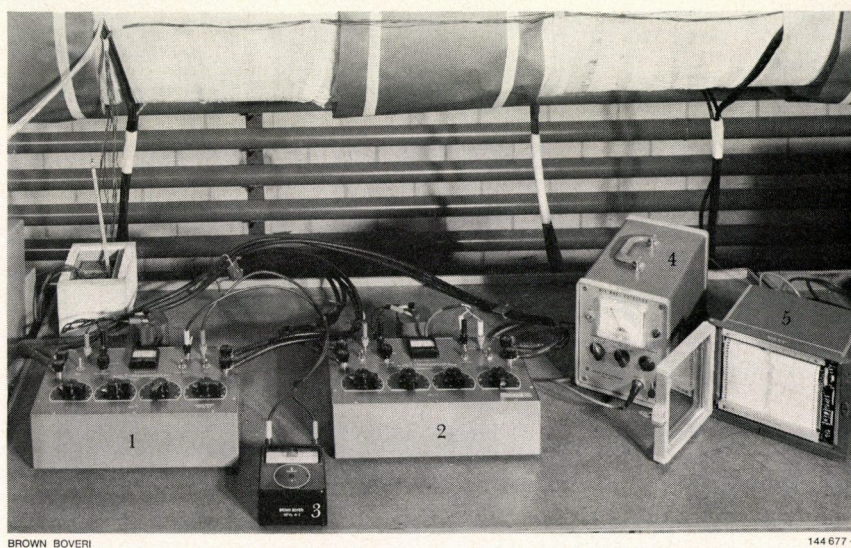
b = fully open

c = symmetrical

d = unsymmetrical

Fig. 5. - Wheatstone bridges and galvanometers for measuring temperature

- 1, 2 = Wheatstone bridges
 3 = Null galvanometer
 4 = Electronic null galvanometer
 5 = Recorder



BROWN BOVERI

144 677-1

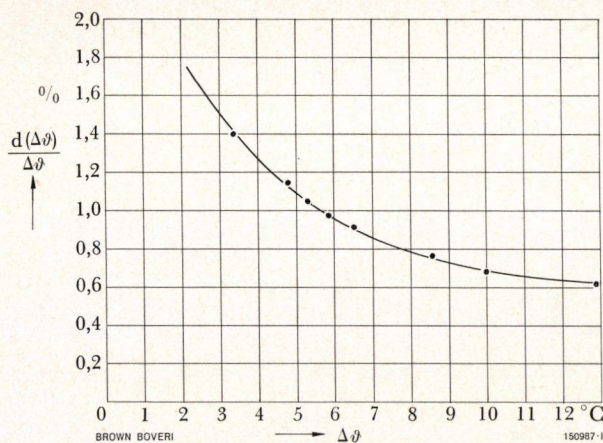


Fig. 6. — Error in determining temperature rise of air in relation to the absolute value $\Delta\theta$

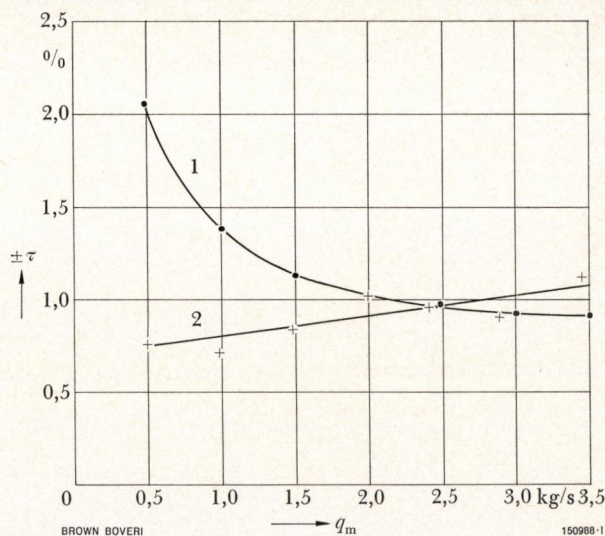


Fig. 7. — Overall tolerance τ of nozzle measurements and calorimetric measurements in relation to the air mass q_m for the series of tests in Table I

- 1 = Nozzle measurements
2 = Calorimetric measurements

far less sensitive to deviations from the ideal velocity profile than corresponding standard nozzle tests.

Errors

The maximum possible (random) error in determining the temperature rise of the air $\Delta\theta$ can be calculated according to the error propagation law:

$$d(\Delta\theta) = \left| \frac{\partial(\Delta\theta)}{\partial a} \cdot da \right| + \left| \frac{\partial(\Delta\theta)}{\partial b} \cdot db \right| + \left| \frac{\partial(\Delta\theta)}{\partial c} \cdot dc \right| + \left| \frac{\partial(\Delta\theta)}{\partial R_{30}} \cdot dR_{30} \right| + \left| \frac{\partial(\Delta\theta)}{\partial(\Delta R_3)} \cdot d(\Delta R_3) \right| + \left| \frac{\partial(\Delta\theta)}{\partial \vartheta_1} \cdot d\vartheta_1 \right| \quad (4)$$

The individual errors da , db and dc were calculated according to the adjustment laws and the remaining components are determined by the following approximations

$$dR_{30} = \pm 0.02 \Omega$$

$$d(\Delta R_3) = \pm 0.02 \Omega$$

$$d\vartheta_1 = \pm 0.3^\circ\text{C}$$

The results of this error calculation are plotted in Fig. 6. The reason for the strong relationship between the error and the absolute value of $\Delta\theta$ lies

in the expression $\frac{\partial(\Delta\theta)}{\partial(\Delta R_3)} \cdot d(\Delta R_3)$.

Whereas this component is only $\pm 0.3\%$ at around $\Delta\theta = 12^\circ\text{C}$, it increases to $\pm 1.2\%$ at about $\Delta\theta = 3^\circ\text{C}$ and where $\Delta\theta$ is even smaller it is almost solely responsible for the total error. For precise measurements therefore, $\Delta\theta$ should never be less than 8 deg C if it can be avoided.

The overall result of the air flow measurements taken by the calorimetric method is a function of $\Delta\theta$, c_{pm} , U and I . If the error limits dc_{pm} , $d(\Delta\theta)$, dU and dI are known or can be estimated, the mean quadratic error of the overall results are given by the following formula:

$$d(q_m)_K = \pm \sqrt{\left(\frac{\partial(q_m)_K}{\partial c_{pm}} \cdot dc_{pm} \right)^2 + \left(\frac{\partial(q_m)_K}{\partial(\Delta\theta)} \cdot d(\Delta\theta) \right)^2 + \left(\frac{\partial(q_m)_K}{\partial U} \cdot dU \right)^2 + \left(\frac{\partial(q_m)_K}{\partial I} \cdot dI \right)^2} \quad (5)$$

The relative value $\tau(q_m)_K = d(q_m)_K/(q_m)_K$ in % is given in Fig. 7, curve 2. The error limits of dc_{pm} , dU and dI are assumed to be $\pm 0.2\%$.

As the thermal output of the heating element could not be raised in line with the increased air throughput, the rise in air temperature dropped from 12 deg C at 1.0 kg/s to about 5 deg C at 3.5 kg/s. The fact that the error increases with q_m , as shown by curve 2 in Fig. 7, is a direct result of this reduction in $\Delta\theta$. For a mean $\Delta\theta$ of about 8 deg C the root mean square error over the complete range from 0.5 to 3.5 kg/s would be less than 1%. It is assumed, however, that for this accuracy in the steady-state condition of air temperature increase, the fluctuations of thermal output and air inlet temperature remain negligibly small.

In [5] the error of calorimetric flow measurement is quoted as ± 2 to 3%. Unfortunately no details are given of the apparatus used or of the air masses involved.

The errors involved in standard nozzle tests are gone into in [2]. As the error in determining the nozzle and duct diameters is small in comparison to the other components, the error calculation according to [1] can be simplified to

$$\tau(q_m)_N = \pm \sqrt{\tau_a^2 + \tau_e^2 + \frac{1}{4}\tau_{\Delta p}^2 + \frac{1}{4}\tau_p^2} \quad (6)$$

In the measurements involved here, τ_e^2 according to [3] is also negligible.

According to [1] the tolerance for the flow coefficient α corresponds to double the estimated standard deviation from a multitude of measured results and this represents a statistical certainty of the α values of 95.4%. It would be safer here to use three times the amount so that the tolerances according to [1] would take on the character of error limits and provide a statistical certainty of 99.7%.

The tolerances of the flow coefficients τ_α are shown in Fig. 1 in relation to the Reynolds number.

In accordance with an error calculation carried out, the tolerance of the density values was considered to be $\tau_\rho = \pm 0.5\%$. The tolerances of the static pressures across the nozzle are considered to be the maximum fluctuations measured at the micromanometer.

These are due partly to the small but unavoidable inconsistencies in fan speed and partly to the air column fluctuations in the connecting tubes to the manometer. Because of this the tolerance $\tau_{\Delta p}$ tended to be too large because each effective pressure measurement was read off as an average value and taken into the calculation.

As stated above the root mean square errors $\tau(q_m)_N$ compiled to form curve 1 in Fig. 7 are derived from air flow masses determined with the aid of standard nozzles.

The reduction in error as the mass of air increases can be traced to component $\frac{1}{4}\tau_{\Delta p}^2$. Whereas at low static pressures τ_a^2 and $\frac{1}{4}\tau_{\Delta p}^2$ are of the same order of magnitude, the static pressure tolerance component of the total error drops as the mass of air increases and at 3.0 to 3.5 kg/s it is negligible with respect to τ_a^2 . With adequately high effective pressures therefore, the accuracy of the nozzle measurements is determined almost solely by the tolerance of the nozzle coefficient. As has already been mentioned, measurements with standard nozzles with an accuracy of $\leq \pm 1\%$ can be made only if the nozzle coefficient for each nozzle used is determined by water calibration.

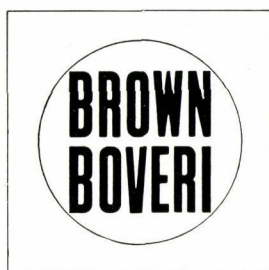
As is illustrated by curves 1 and 2 in Fig. 7 the error calculations for both measuring methods gave root mean square errors $\tau(q_m)$ of the same order of magnitude.

(AH)

H. STRUPP

Bibliography

- [1] Draft DIN 1952. Durchflussmessung (Flow measurement). Dec. 1963 (7th edn).
- [2] The measurement of fluid flow by means of orifice plates and nozzles. ISO Recommendation R 541, 1967.
- [3] F. HERNING: Grundlagen und Praxis der Durchflussmessung. VDI Verlag, 1967, 3rd edn, p. 34-5 and 77-82.
- [4] H. STRUPP: Air calorimetry of open-type machines. Brown Boveri Rev. 1968, Vol. 55, No. 10/11, p. 640-9.
- [5] J. HAK: Strömungstechnische Untersuchung elektrischer Maschinen mittels der luftdichten Kammer. Elektrotech. u. Maschinenb. 1962, Vol. 79, No. 15/16, p. 395-9.



Published by Brown, Boveri & Company, Limited, Baden, Switzerland. Printed by Berichthaus Zurich, Switzerland.

Obtainable direct from the publishers